

AIR FORCE  
BALLISTIC MISSILE DIVISION

TECHNICAL LIBRARY

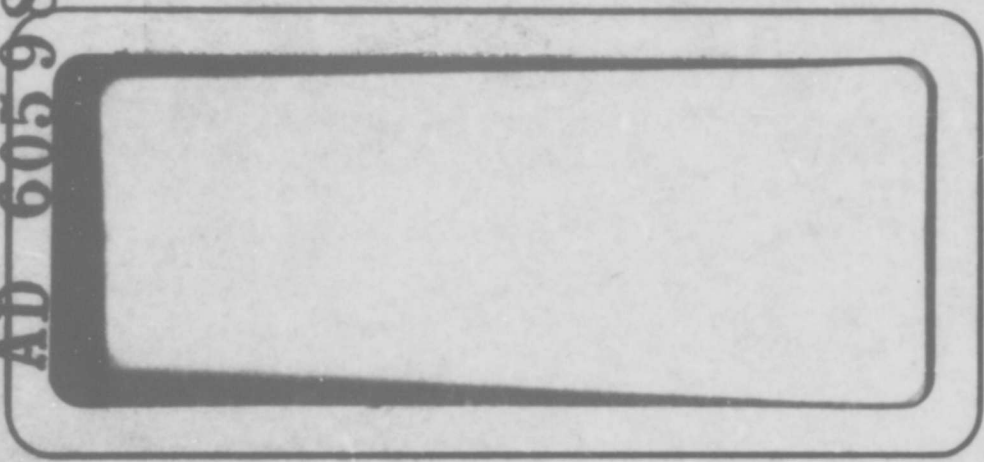
Document No. 60-12-9017

Copy No. 1/2

①<sup>12</sup>

AD-  
605984

AD 605984



COPY <u>1</u> OF <u>1</u>	
HARD COPY	\$.
MICROFICHE	\$.



**DO NOT PHOTOGRAPH THIS PAGE**

SPACE TECHNOLOGY LABORATORIES, INC.

DDC  
RECEIVED  
SEP 29 1964  
RESOLVED  
DDC-IRA E

60129017

H

AD 605984

COPY	1	OF	1	unit
HARD COPY		\$.	3.00	
MICROFICHE		\$.	0.75	

78p

LOW PRESSURE  
ELECTRICAL DISCHARGE STUDIES

By  
W. H. Krebs and A. C. Reed


STL/TR-59-0000-09931

17 December 1959

Contract No. AF 04(647)-309

Approved:

  
L. K. Lee, Manager  
Product Engineering Department

  
W. T. Russell, Director  
Electromechanical Laboratory


SPACE TECHNOLOGY LABORATORIES, INC.  
P. O. Box 95001  
Los Angeles 45, California

  
ABSTRACT

<sup>T<sub>11</sub></sup>  
~~This~~ report concerns electrical breakdown of air at low pressures or high altitudes (70,000 to 250,000 feet) due to secondary emission. Information pertinent to the problem of low frequency (0 to 1000 cps) sparking was compiled through a literature survey. A bibliography concerning electrical breakdown at both low and high frequencies was compiled.

A test program ~~conducted in the Environmental Evaluation Section of Space Technology Laboratories, Inc.~~ yielded the following results: no statistically significant deviation from Paschen's Law was detected. The addition of water vapor to the air constituting the test environment caused a significant lowering of the minimum sparking voltage.

Recommendations are made relative to test programs for missile electrical components employing voltages higher than 200 volts. ( )



## SUMMARY

Electrical breakdown of gases has caused various malfunctions in missiles flying through the earth's atmosphere. A bibliographical and experimental study of the phenomena causing these malfunctions was initiated at Space Technology Laboratories. This report presents some of the pertinent facts concerning these phenomena and how they apply to missile design.

The literature survey indicated that breakdown at the low air pressures (70,000 to 250,000 feet of altitude) is best accounted for by secondary emission considerations. Paschen's Law is based on these considerations. This law is important because, within certain limitations, it can be used to predict pressures at which breakdown of a gas between uninsulated clean electrodes may occur. Testing was conducted in the STL laboratory to ascertain whether Paschen's Law remained valid for gap spacings from 2 mm to 70 mm. No deviation was detected by statistical analysis of the data.

The published minimum sparking voltage of 324 volts at a pressure-distance product of 5.67 mmHg-mm is in good agreement with STL test results. These results indicated that, with dry air, the minimum voltage was 385 volts at 6 mmHg-mm; with "wet" air, the minimum voltage was 335 volts at 6 mmHg-mm. The minimum voltage encountered in an experiment using MS type electrical connectors was 365 volts peak occurring at a pressure predicted by Paschen's Law. These measurements were made using frequencies of 60, 400 and 1000 cps.

These voltages are higher than the recommended maximum instantaneous operating voltage difference of 200 volts for missiles. This 200 volt criterion was established because it is the lowest voltage at which a glow discharge can be maintained using materials which are incorporated in missile hardware. It also provides a safety margin to allow for other mechanisms which can reduce the breakdown voltage between two terminals.

Another phase of the testing at STL demonstrated that if two possible discharge paths existed within a conducting cylinder, one path being longer than the other, the discharge will follow the longer of the paths if the pressure is

reduced below some critical value. This implies that an electrical discharge within a missile could start between two closely spaced electrodes and then shift to another electrode spaced further away as the pressure is reduced below some critical value. Information pertinent to the power dissipated in the gap is included in the report.

Confusion as to the nomenclature describing some aspects of secondary emission exists; this report contains some statements correlating and clarifying some of this nomenclature. Arcing is a phenomenon which is explained by thermionic theory and not by secondary emission theory. The two disciplines describe different aspects of the conduction of electricity in gases. Means of reducing the possibility of voltage breakdown in missile applications are discussed.

Different geometrical configurations were considered both in the literature survey and in the testing. It required a higher voltage to break down the point-to-point electrode space than to break down the parallel-plane electrode space at the low pressures under consideration. It was also determined that if a wire within an enclosed cylinder is made positive with respect to the cylinder, then the breakdown voltage will be higher than if the wire is negative with respect to the cylinder.

Basic considerations and a mathematical treatment of secondary emission phenomena are included in Appendix I. A pressure-to-altitude conversion chart appears as Appendix II. An outline of the statistical method used to arrive at the conclusion that no detectable statistical deviation from Paschen's Law existed is outlined in Appendix III.

Means of preventing voltage breakdown, such as the use of encapsulation, potting, and vacuum-cast materials are discussed. A bibliography of articles on voltage breakdown at high and low frequencies is included.

## CONTENTS

	Page
I. INTRODUCTION . . . . .	1
II. PURPOSE . . . . .	1
III. BACKGROUND AND THEORETICAL CONSIDERATIONS . . . . .	2
IV. TEST EQUIPMENT . . . . .	7
V. TEST SETUP . . . . .	8
VI. TEST PROCEDURE . . . . .	11
VII. TEST RESULTS . . . . .	13
A. Parallel Plane Electrodes . . . . .	13
B. Pointed Electrodes . . . . .	19
C. Long-Gap Discharge . . . . .	22
VIII. DISCUSSION AND RECOMMENDATIONS . . . . .	24
APPENDIX I . . . . .	36
A. Electric Current in Gases . . . . .	36
B. Townsend's Equation . . . . .	38
C. Townsend's Criterion for Sparking . . . . .	42
D. Paschen's Law . . . . .	46
E. Nonuniform Electric Field . . . . .	49
F. Electrode Material and Gas Composition . . . . .	52
G. Cathode Potential Fall . . . . .	53
APPENDIX II . . . . .	56
Altitude-Pressure Conversion Table . . . . .	56
APPENDIX III . . . . .	57
A. Linear Regression . . . . .	57
B. Prediction Interval for the Regression Line . . . . .	59
C. Statistical Test of Hypothesis on the Regression Slope . . . . .	60
D. Confidence Limits for the Regression Slope . . . . .	61
BIBLIOGRAPHY . . . . .	62
ACKNOWLEDGEMENT . . . . .	64

## ILLUSTRATIONS

Figure		Page
1	Schematic Characteristic of a Gas Discharge Between Flat Parallel Plates . . . . .	3
2	Circuit for Determination of Sparking Voltage Using Rogowski Surface and Conical Shaped Electrodes . . . . .	9
3	Circuit Used for Long Gap Discharge Study . . . . .	9
4	Rogowski Surfaces . . . . .	10
5	Long Gap Discharge Chamber . . . . .	10
6	Pointed Electrodes . . . . .	12
7	Statistical Test for Deviations from Paschen's Law $V = K = 415$ Volts (R. H. Portion of Breakdown Voltage Curve . . . . .	15
8	Statistical Test for Deviations from Paschen's Law $V = K = 415$ Volts (L. H. Portion of Breakdown Voltage Curve . . . . .	16
9	Short Gap Discharge Study – Comparison of Breakdown Voltages with Respect to Gap Aperture . . . . .	17
10	Short Gap Discharge Study – Comparison of Breakdown Voltages with Respect to Gap Aperture . . . . .	18
11	Short Gap Parallel Plane Discharge Study – Comparison of Breakdown Voltages . . . . .	20
12	Short Gap Discharge Study – Comparison of Breakdown Voltages . . . . .	21
13	Long Gap Discharge – Sparking Voltage Versus Pressure . . . . .	23
14	Long Gap Discharge – Gap Voltage Versus Applied Voltage . . . . .	25
15	Long Gap Discharge – Total Power into Circuit . . . . .	26
16	Long Gap Discharge – Percentage of Power Input Dissipated in the Gap. . . . .	27
17	Long Gap Discharge – Total Power into Circuit. . . . .	28
18	Long Gap Discharge – Percentage of Power Input Dissipated in the Gap. . . . .	29
19	Long Gap Discharge – Current Versus Applied Voltage. . . . .	30
20	Long Gap Discharge – Current Versus Applied Voltage. . . . .	31
I-1	Current in an Ionization Chamber with Increasing Voltage . . . . .	37
I-2	Ionization by Collision . . . . .	39
I-3	Typical Breakdown Voltage Curves for Different Gases Between Parallel Plate Electrodes Illustrating Paschen's Law . . . . .	47
I-4	Breakdown Voltage Curves for Different Cathode Materials in Hydrogen . . . . .	53

## I. INTRODUCTION

This report is concerned with the electrical breakdown of air at low gas pressures (20 microns to 40 mm Hg) resulting primarily from secondary emission phenomena. Information was obtained both from a survey of the literature on the subject and from a laboratory testing program. The results of the laboratory testing program using parallel plane electrodes were subjected to statistical tests of significance.

## II. PURPOSE

The purpose of the literature survey was to locate theoretical information and test data relating to the following subjects:

- a) the phenomena causing electrical breakdown in air at low pressures;
- b) the minimum value of the voltage required for a self-sustained electrical discharge in air at low pressures;
- c) the pressure-distance product (pd) at which the minimum breakdown voltage value for electrical breakdown of air at low pressure is observed.

A secondary objective of the literature survey was to compile a bibliography on the topic of electrical breakdown to serve as a reference source for more detailed information on various aspects of the phenomenon.

The purposes of the laboratory testing program were:

- a) to determine whether a properly designed test could detect statistically significant deviations from Paschen's Law
- b) to determine whether such significant deviations were in the direction of higher breakdown voltages, thus the predictions of Paschen's Law would be lower than that voltage actually required to break down the gap
- c) to ascertain qualitatively the effect of humidity on the minimum voltage required for electrical breakdown at low gas pressures

- e) to verify and demonstrate with special long-gap discharge apparatus that, where there are two possible discharge paths of different length, the discharge will follow the longer of the paths when the pressure is reduced below some critical value
- f) to obtain power dissipation data with the long-gap discharge apparatus.

### III. BACKGROUND AND THEORETICAL CONSIDERATIONS

Electrical breakdown of gases has caused various malfunctions in missiles flying through the earth's atmosphere. This electrical breakdown of air between uninsulated wiring occurs generally at low atmospheric pressures (1 micron Hg to 100 mm Hg). These breakdowns are due to secondary emission. This phenomenon occurs when positive ions attain enough velocity due to the applied electric field to knock electrons out of the negative electrodes. When this occurs, the discharge is termed self-sustained (see following paragraph). The transition from a nonself-sustained discharge to any of the self-sustained discharges is called sparking.

The saturation current and all currents having a lower magnitude are non-self-sustained discharges. The saturation current is a current between two electrodes composed of all the ions formed by an external ionizing source; all these ions are drawn to the electrodes by the applied field before any of the ions can recombine within the gap. When this condition is reached, a further increase of voltage causes no increase in current until the voltage approaches the sparking threshold. If the ionizing source were removed, the magnitude of current would drop to zero. But once the sparking voltage has been applied, the current becomes self-sustained in the absence of any external ion source.

The self-sustained discharges have been divided into different categories according to their characteristics. The Townsend Spark Discharge has the lowest value of current of the self-sustained discharges. This discharge (Region 1, Figure 1) is sometimes referred to as the dark discharge (Reference 9, XXII, p. 54). The volt-ampere curve has both a positive slope and a zero slope in this region. The current density is below  $10^{-6}$  amperes per square centimeter (when using parallel plane electrodes) thus the field is not distorted due to space

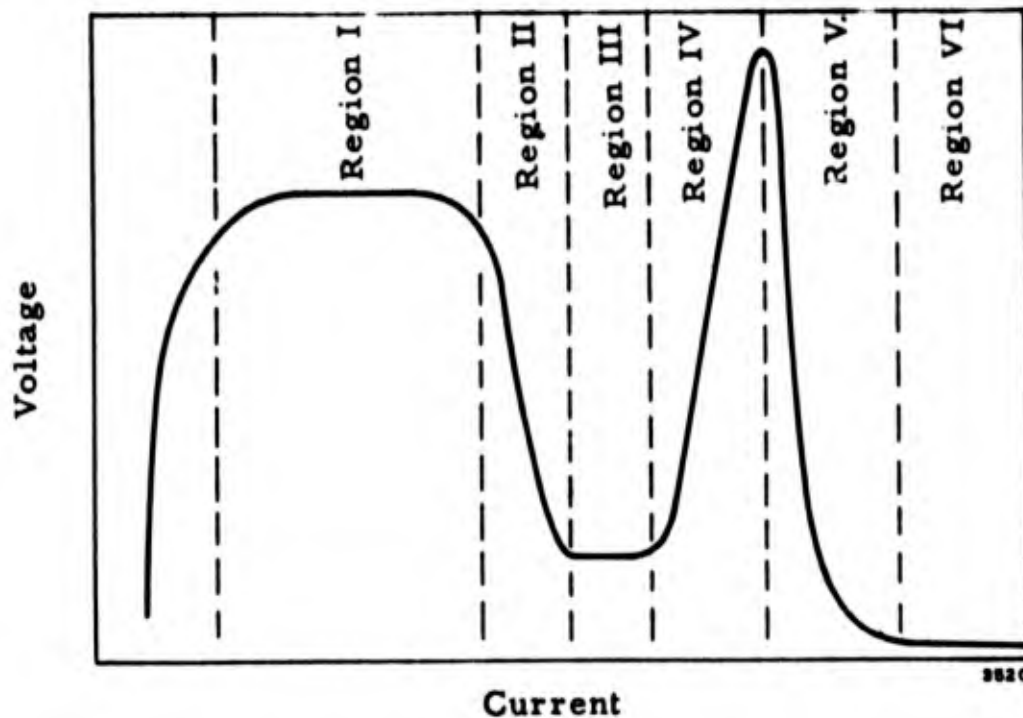


Figure 1. Schematic Characteristic of a Gas Discharge Between Flat Parallel Plates.

charges. In all subsequently named discharges, the current density will be higher than this critical value and, therefore, the field will be distorted. When the current is increased slightly, the slope of the volt-ampere curve becomes negative (Region II, Figure 1). This discharge is called the transition current by some (Reference 15, p. 127) and by others, the dark current (Reference 9, XXI, p. 574) because it is not visible to the eye under normal conditions. Yet another author labels the discharge in this region the corona and subnormal glow discharges (Reference 9, XXII, p. 54). This corona is a transient-type discharge. The current flow is intermittent and the frequency of the current which does flow is not necessarily that of the applied voltage. If the current is again increased slightly, the slope of the volt-ampere curve is approximately zero (Region III, Figure 1) and the discharge becomes visible. If this visible discharge only partially covers the cathode, it is termed a normal glow discharge. The voltage necessary to maintain this discharge is much less than the voltage necessary to produce sparking. In engineering situations, the normal glow discharge is often incorrectly called corona. If the current is again increased slightly, the

area of the glow discharge on the cathode will grow until the entire cathode electrode area is enveloped by a glow (Region IV, Figure 1). This is called the "abnormal" or anomalous glow discharge. The voltage necessary to maintain this phenomenon is always higher than the voltage required for the normal glow discharge and may exceed the sparking voltage. As the gap voltage increases in this region, the current density also rises. If the current is again increased slightly, the slope of the volt-ampere curve becomes negative (Region V, Figure 1) until arcing occurs (Region VI, Figure 1). The slope of the volt-ampere curve after initiation of the "arc discharge" is almost zero. The voltage necessary to maintain the arc is very much lower than that needed to maintain even the normal glow discharge. The arc discharge is characterized by the high temperature of the electrodes. In all cases the electrodes are at the boiling temperature for the materials used. The arc discharge may be described quantitatively by the mathematics developed for thermionic emission. The mathematical equations developed using secondary emission concepts, which with modification apply to the glow discharges, do not apply to arc discharges. The glow discharges are "cold cathode" phenomena whereas the arc discharge is a hot cathode phenomenon.

The magnitude of current necessary to obtain these discharge characteristics is determined by the given gas, gas pressure, and electrode geometry, as well as by external circuitry.

The mathematical considerations necessary for sparking to take place were originally developed by J. S. Townsend. The following equation was developed by Townsend to describe the current flow in the gap, considering only secondary emission phenomena.

$$i = i_0 \frac{\epsilon^{ad}}{1 - \gamma(\epsilon^{ad} - 1)}$$

where

- $i$  = current in the gap
- $i_0$  = saturation current
- $\gamma$  = average quantity of electrons emitted from the cathode for each positive ion bombarding the cathode

$\alpha$  = number of new pairs of ions formed by collision per unit distance of travel by an existing free electron

$d$  = the distance between planar, parallel electrodes.

From this equation has come the criterion for sparking. This occurs when the mathematical expression for  $i$  becomes infinite. The criterion is expressed as follows:

$$\gamma (\epsilon^{\alpha d} - 1) = 1$$

This criterion is true within certain limitations. Some of these limitations are expressed by Von Engel (Reference 27, p. 149). Accurate numerical values of  $\gamma$  expressed as a function of  $E/p$  (ratio of electric field strength to gas pressure) for air have not been agreed upon for low values of  $E/p$ . Experimental and theoretically predicted values do not agree. It is also noted that gamma ( $\gamma$ ) will have a value which is characteristic of neither metal when a thin film of some metal is deposited on a cathode of another material. The value of gamma is sometimes higher and sometimes lower than that measured when the metals are used by themselves (Reference 9, XXI, p. 600). This is true even when the field strength/pressure quotient is high enough to ensure adequate measurements of gamma. The value of gamma is very dependent on the material of the electrodes, the surface condition of the electrodes, and the purity of the air. This makes it imperative that one use published values of gamma with discretion when applying mathematical formulae to predict sparking conditions for given electrode configurations and given materials as occur in engineering situations. If one uses a pure gas medium, the theoretical and experimental data agree fairly well.

Paschen's Law, often referred to as the law of similarity, is an experimental fact discovered by Paschen in 1889 (Reference 4, p. 163). It states that the sparking potential is a function only of the product of pressure and gap length. Paschen's Law is important because it can be used to predict approximately the pressure at which sparking will occur when fairly uniform field conditions exist and the gap distance and pressure-distance product for that sparking voltage are known.

Paschen's Law can be derived from the more fundamental Townsend sparking criterion. A mathematical derivation and treatment of Townsend's equations and Paschen's Law may be found in Appendix I, which is a major portion of the preliminary literature study (Reference 22, pp. 4-20).

The published minimum sparking potential for steel parallel-plane electrodes, as derived from experiments using air, is in the 324 to 330 volt range (Reference 15, p. 92 and Reference 4, p. 165) for a pd of approximately 6 mmHg-mm.

One published value of minimum sparking voltage using carbon electrodes is 350 volts (Reference 5, pp. 562-563) at a pd of 6 mmHg-mm.

The published value of the pd product for the minimum sparking voltage, a measure of the number of molecules in the gap, is 5.67 to 6.0 mmHg-mm spacing. A sparking curve based on previously published material may be found in Appendix I. This value of pd is not greatly affected by the materials used for the electrodes. For purposes of converting pressure values to altitude values, see Appendix II.

From bibliographic material pertinent to the sparking problem, it is deduced that the sparking voltage curve at low pressure levels is not appreciably changed from the direct-current values if frequencies in the 0 to 1000 cps range are used. Results of testing by Convair (Reference 21) on standard military electrical connectors indicated that the minimum corona initiation voltage was 365 volts peak using power supply frequencies of 60, 400, and 1000 cps. The effect which the Convair report called corona probably was a glow discharge and thus their "initiation voltage" was actually a sparking voltage.

When electrical breakdown between a wire and a coaxial cylinder is considered, the voltage for sparking is minimum when the wire is negative with respect to the coaxial cylinder. According to a diagram shown by Meek and Craggs (Reference 15, p. 102), if the wire is negative, the minimum sparking voltage is 370 volts, and if the wire is positive, the minimum sparking voltage is 500 volts. The former value agrees fairly well with the 365 volts peak recorded in the Convair experiment using an MS connector (Reference 21, p. 2).

The literature on the effect of placing a dielectric material between the electrodes was also surveyed. It is generally acknowledged that this process may reduce the value of the minimum voltage needed for sparking. This occurs because the effects of layers of gas, moisture and dust may form an alternate path for the current (Reference 4, p. 166).

An interesting form of glow discharge, called the "spray discharge" (Reference 9, XXII, p. 634) results when a dielectric is placed on the cathode. A cathode of carbon or aluminum covered by an insulating layer or powder (e. g.,  $Al_2O_3$ ) can maintain a discharge at a cathode fall voltage of less than 40 volts with current densities thousands of times larger than those found in the glow discharge (Reference 9, XXII, p. 634 and Reference 25, pp. 1704-1712). The normal cathode fall potential for aluminum in that gas is much higher. This phenomenon is being made use of in cold cathode vacuum tubes.

It should be noted that the magnitude of the voltage needed to produce sparking in nitrogen is approximately 251 volts, and for hydrogen is 273 volts. The pd product for the minimum sparking voltage in nitrogen is 6.7 mmHg-mm, and for hydrogen is approximately 11.5 mmHg-mm (Reference 4, p. 165). (It is assumed that these values are quoted for stainless steel electrodes.)

#### IV. TEST EQUIPMENT

- 1) Autovac Gauge, Consolidated Electrodynamics Corp., Type 3294B with Pirani Gauges, SN B294B418.  
Accuracy  $\pm 5\%$  of scale reading
- 2) Bell Jar Chamber, Cenco, Model 94212 with a Hyvac 7 pump.
- 3) Gas Drying Unit, W. A. Hammond Drierite Co. Desiccant material is anhydrous calcium sulfate.
- 4) Long-Gap Discharge Chamber, STL designed. (See Figure 5.)
- 5) Microammeters, Weston Model 1721  
Accuracy  $\pm 2\%$

- 6) Microammeter, Sensitive Research Inc., Model "University"  
No. 906205.

Accuracy  $\pm 0.5\%$

- 7) Power Supply Regulated, Electronic Measurements Co.,  
Model 207B, SN540.

- 8) Voltmeter, Weston Model 931, SN40450

Accuracy  $\pm 0.5\%$

## V. TEST SETUP

An "Autovac" Pirani gauge was used for pressure measurements. The Autovac gauge senses the change of resistance of a filament due to the cooling effect of the gas. Two resistance elements were monitored during any given test run, thus checking each other. During the testing period, the Pirani resistance elements were calibrated by the use of a McLeod vacuum gauge. Within the pressure range covered, the error of the Autovac gauge was within the allowable tolerance specified by the instrument manufacturer.

The electrical quantities of voltage and current were measured by a Weston Model 931 voltmeter, and two Weston center scale zero-type microammeters -- for the circuitry, see Figures 2 and 3. The microammeters were calibrated against a Sensitive Research microammeter used as a secondary standard. The readings of the microammeters were corrected using the calibration curves. The voltmeter was calibrated against another secondary standard in the Instrument Center of Space Technology Laboratories.

The bell jar and the long-gap discharge chamber were utilized to provide the vacuum. Pictures of these units may be seen in Figures 4 and 5. The structure beneath the bell jar, and the metal hood over the bell jar were kept at ground potential.

For determination of deviations from Paschen's Law, a pair of Rogowski surface type electrodes (called parallel plates in the literature) made from stainless steel were used. These surfaces are so designed, that for a given gap distance the radius of curvature for the edges of the electrodes follows voltage

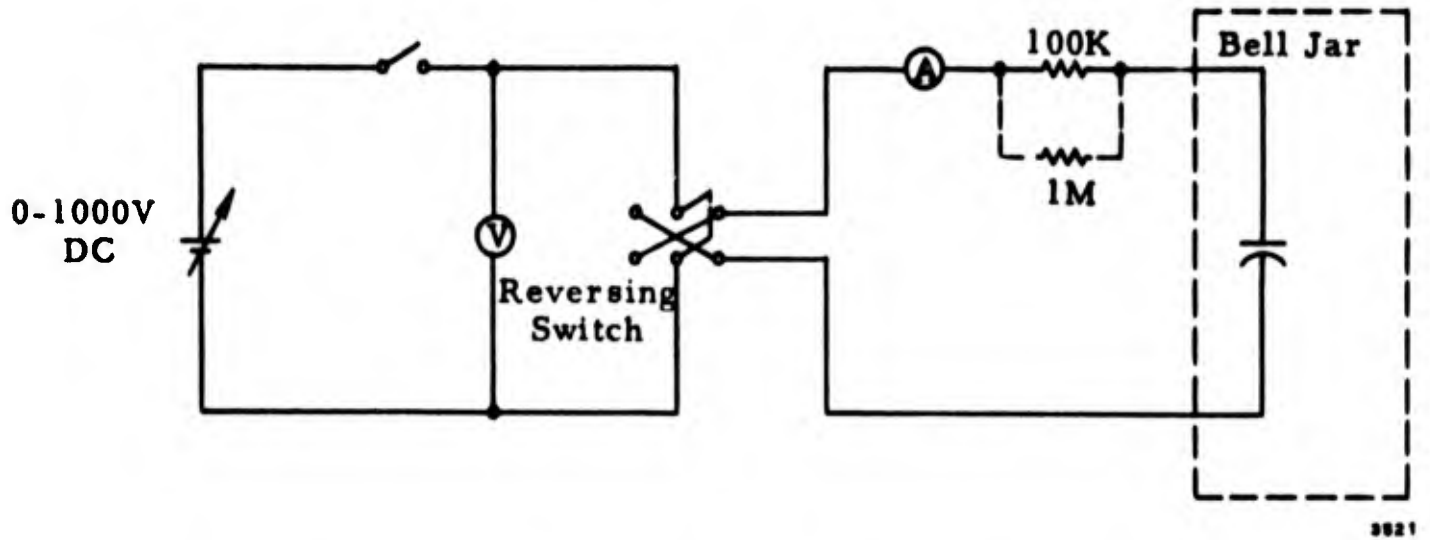


Figure 2. Circuit for Determination of Sparking Voltage Using Rogowski Surface and Conical Shaped Electrodes.

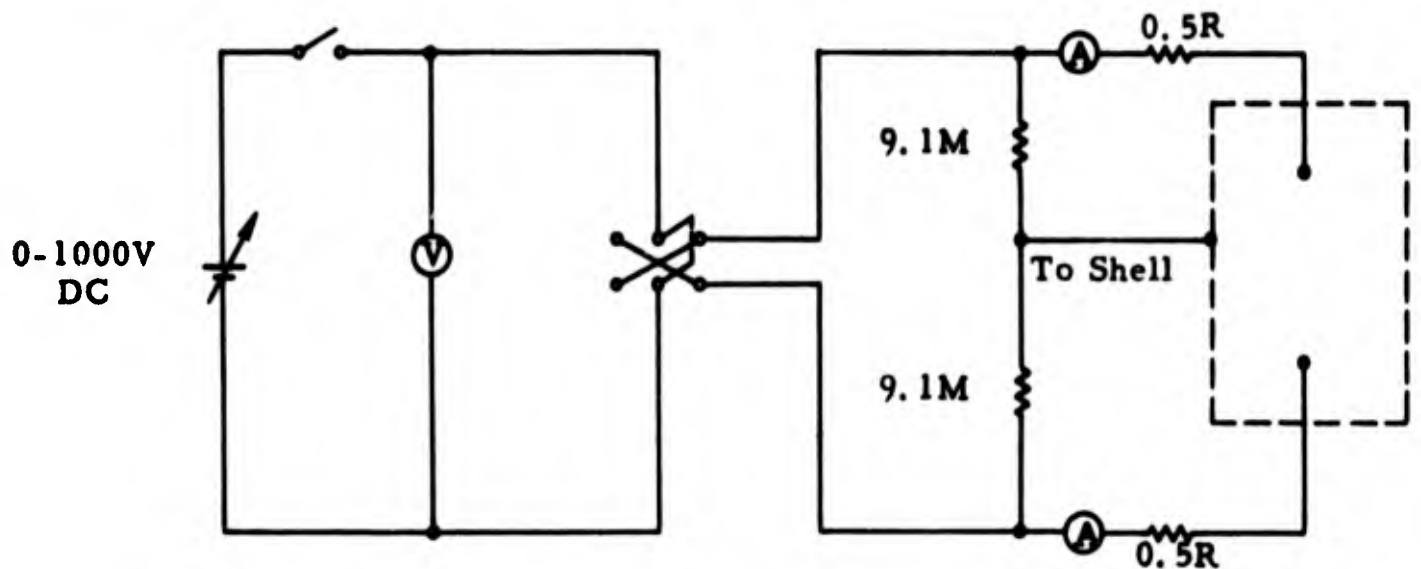


Figure 3. Circuit Used for Long Gap Discharge Study.



1468

Figure 4. Rogowski Surfaces.



1470

Figure 5. Long Gap Discharge Chamber.

equipotential surfaces as defined by Rogowski's extension of Maxwell's analysis of the electrostatic field between a finite plane plate and a parallel infinite plane plate (Reference 4, p. 177). If the equipotential surfaces are so-called  $\pi/2$  or lower-valued surfaces, then according to Rogowski, the voltage gradient between plane portions of the electrodes is always greater than the gradient outside of the plane portions of the electrodes. Rengier has experimentally found that for electrodes following the dimensions of a  $2\pi/3$  surface, the sparking always occurred within the plane portion of the electrodes. The Rogowski surfaces used in the testing program were  $\pi/2$  surfaces at a spacing of 2 millimeters and  $2\pi/3$  surfaces at the 5 millimeter spacing. At distances greater than these, the surfaces approximate flat plates, thus introducing edge effects which cause higher field gradients to appear at the outer edges of the electrodes rather than between the plane portions.

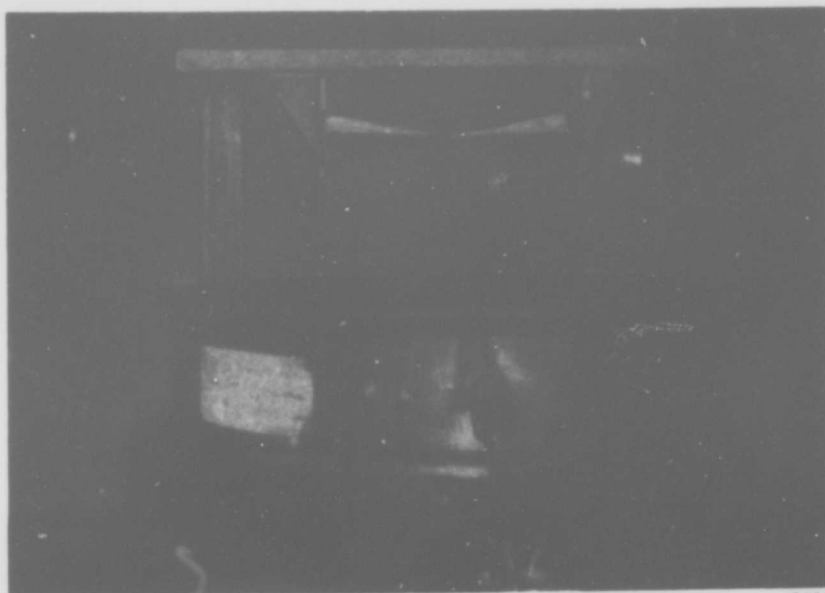
These Rogowski-type electrodes were polished until the grain of the material was evident to the unaided eye. Before the electrodes were subjected to altitude, all exposed metal wiring between the electrodes and the bell jar terminals was sprayed with "acrylic" - a plastic insulation. The electrodes were mounted as illustrated in Figure 4.

The electrodes for the long-gap discharge (Figure 5) testing were made of brass. The shape of these electrodes may be described as a spheroid placed on a long slender column. The outer shell of the long-gap discharge chamber was made of aluminum.

The pointed electrodes were composed of stainless steel. They were cones having a tip angle of  $15^\circ$ . These are shown in Figure 6.

## VI. TEST PROCEDURE

To obtain repeatable and consistent data, a definite procedure in admitting air to the bell jar had to be followed. The chamber pressure had to be reduced to below 25 microns and held there for approximately two hours; then air was introduced into the vacuum chamber for approximately five minutes before beginning the experiment. The pressure was then slowly increased or decreased, holding the voltage constant until the occurrence of an electrical discharge was indicated by a microammeter.



1469

Figure 6. Pointed Electrodes.

To form the basis for a statistical analysis of data, a minimum of ten observations of pressure was made for each voltage and spacing combination. At least nine voltage points per sparking voltage curve were taken. A sparking voltage curve was taken for each of the following spacings: 2, 5, 10, 30 and 70 mm. The effect of voltage polarity was observed by taking five observations with one electrode being negative and then taking five observations after switching polarity. A sparking voltage curve was also taken for the pointed electrodes which were at a 2 mm spacing.

Accurate positioning of the electrodes was accomplished by the use of gauge blocks, thus ensuring that the plane portions of the Rogowski surfaces would be parallel and separated by the desired distance.

To obtain dry air in the vacuum chambers, air was drawn through a gas drying unit filled with anhydrous calcium sulphate. Moist air was obtained by drawing air of high relative humidity (>50 percent relative humidity) from an enclosed container.

The data for the long-gap discharge sparking curve were obtained by holding the pressure constant and slowly increasing the voltage until an electrical discharge took place. The data for power measurements were taken by increasing the voltage to sparkover and then setting it to voltage level desired for making current measurements. At the pressure of 45 microns Hg, great care had to be exercised in obtaining the current because an upward shift of 2 microns of pressure would cause a 10 percent increase in current. The circuitry for obtaining the power measurements using the long-gap discharge chamber is shown in Figure 3. The aluminum shell potential was midway between the electrode potentials. The power dissipated in the gap was varied by changing the values of the series resistors. The values of the series resistance used were 60,000, 120,000, 480,000, 1,200,000 and 2,000,000 ohms.

## VII. TEST RESULTS

### A. Parallel Plane Electrodes

A statistical analysis of the data for dry air, indicated no significant deviations from Paschen's Law even at the greater spacings where the field was not uniform. Table 1 and Figures 7 and 8 illustrate this point. Table 1 gives the slope of each set of data taken for a constant voltage setting, and the results of the statistical significance tests. The statistical approach for determination of the table values is outlined in Appendix III. The approach of testing Paschen's Law by the statistical means is outlined in Appendix I. A preliminary statistical study indicated that there were deviations. Unfortunately, some of the data points chosen for this preliminary statistical study were from dissimilar populations; sample data points were derived from tests involving both "wet" and "dry" air.

The  $pd$  product range for both dry and wet air at which the minimum sparking voltage occurred was between 5.6 and 6.3 mmHg-mm. See Figures 9 and 10. This agrees fairly well with the published average value of 5.67 mmHg-mm spacing.

**BLANK PAGE**

Significance Tests for $-m/n$												
Voltage	Sample Size	$-m/n$	T	$t_{n-2, 0.90}$	Significance	Confidence Limits	$t_{n-2, 0.95}$	Significance	Confidence Limits	$t_{n-2, 0.99}$	Significance	Confidence Limits
400R	52	0.997	0.241	1.676	No	0.977-1.017	2.009	No	0.973-1.021	2.678	No	0.965-1.029
400L	34	0.964	1.914	1.694	Yes	0.932-0.996	2.038	No	0.926-1.002	2.741	No	0.912-1.016
415R	75	1.019	1.840	1.667	Yes	1.002-1.036	1.993	No	0.998-1.040	2.646	No	0.992-1.046
415L		0.993	0.272	1.671	No	0.987-1.053	2.001	No	0.940-1.046	2.662	No	0.922-1.064
425R		1.001	0.087	1.669	No	0.984-1.018	1.997	No	0.980-1.022	2.654	No	0.973-1.029
425L	50	1.020	1.001	1.678	No	0.986-1.018	2.011	No	0.980-1.060	2.683	No	0.967-1.073
450R	77	1.003	0.320	1.666	No	0.988-1.018	1.992	No	0.985-1.021	2.644	No	0.979-1.027
500R	76	0.994	1.014	1.666	No	0.982-1.006	1.993	No	0.980-1.008	2.645	No	0.975-1.013
600R	72	0.995	0.626	1.667	No	0.981-1.009	1.995	No	0.979-1.011	2.641	No	0.973-1.017

Table 1. Statistical Tests for Deviation of Slope from -1,  $\log p = -m/n \log d + K (V_s)$

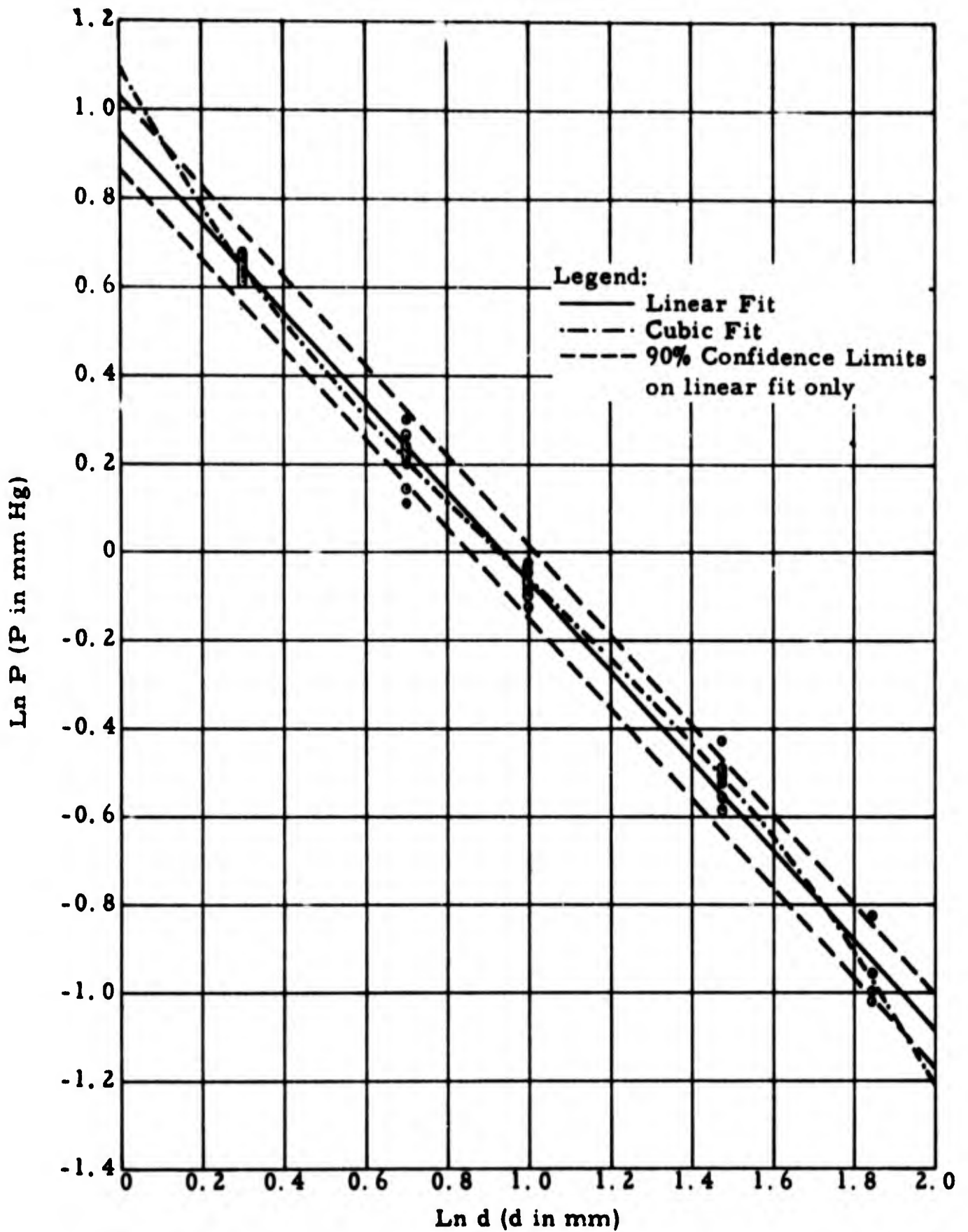


Figure 7. Statistical Test for Deviations from Paschen's Law.  $V = K = 415$  Volts (R. H. Portion of Breakdown Voltage Curve).

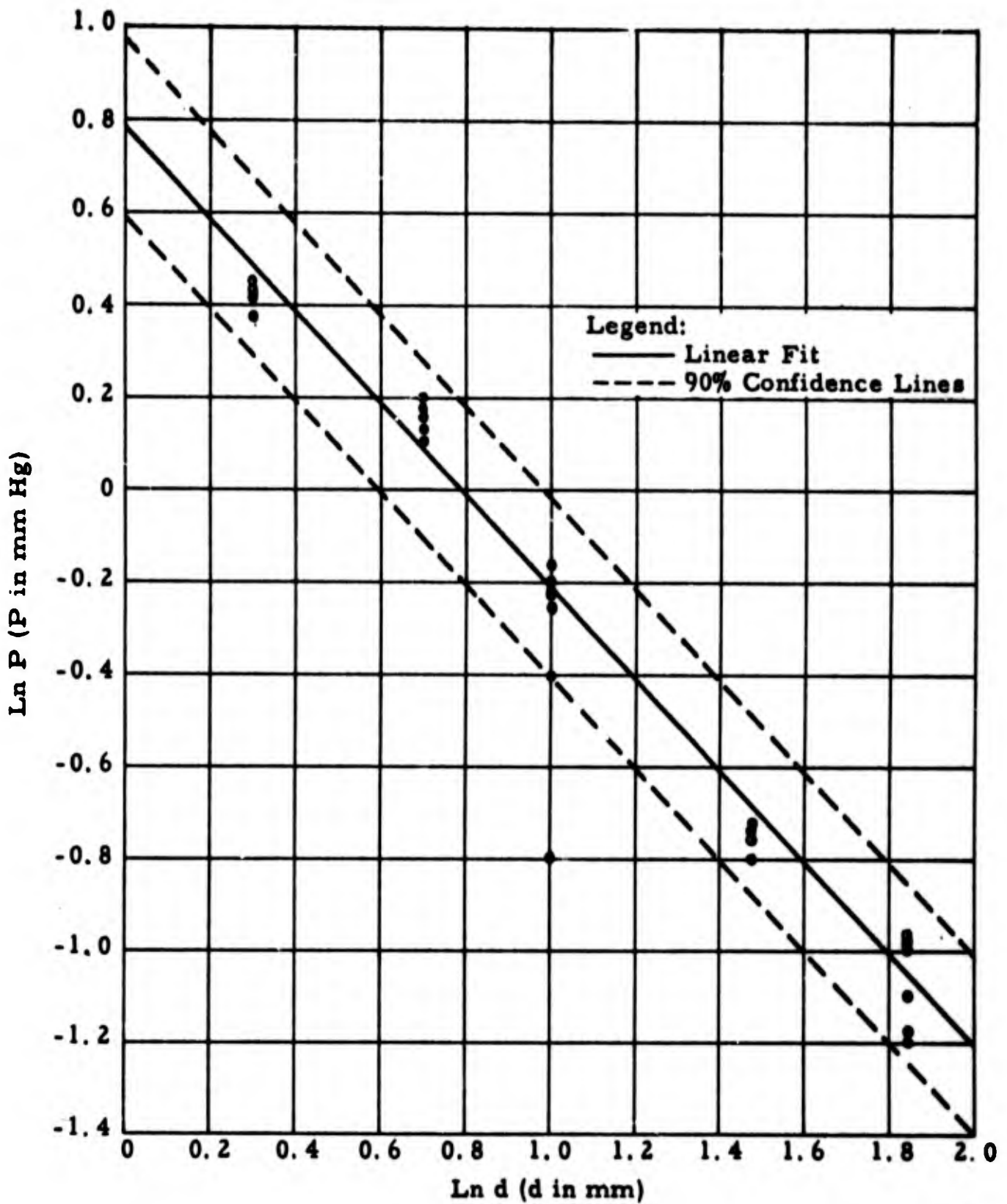


Figure 8. Statistical Test for Deviations from Paschen's Law.  
 $V_s = K = 415$  Volts (L. H. Portion of Breakdown  
Voltage Curve).

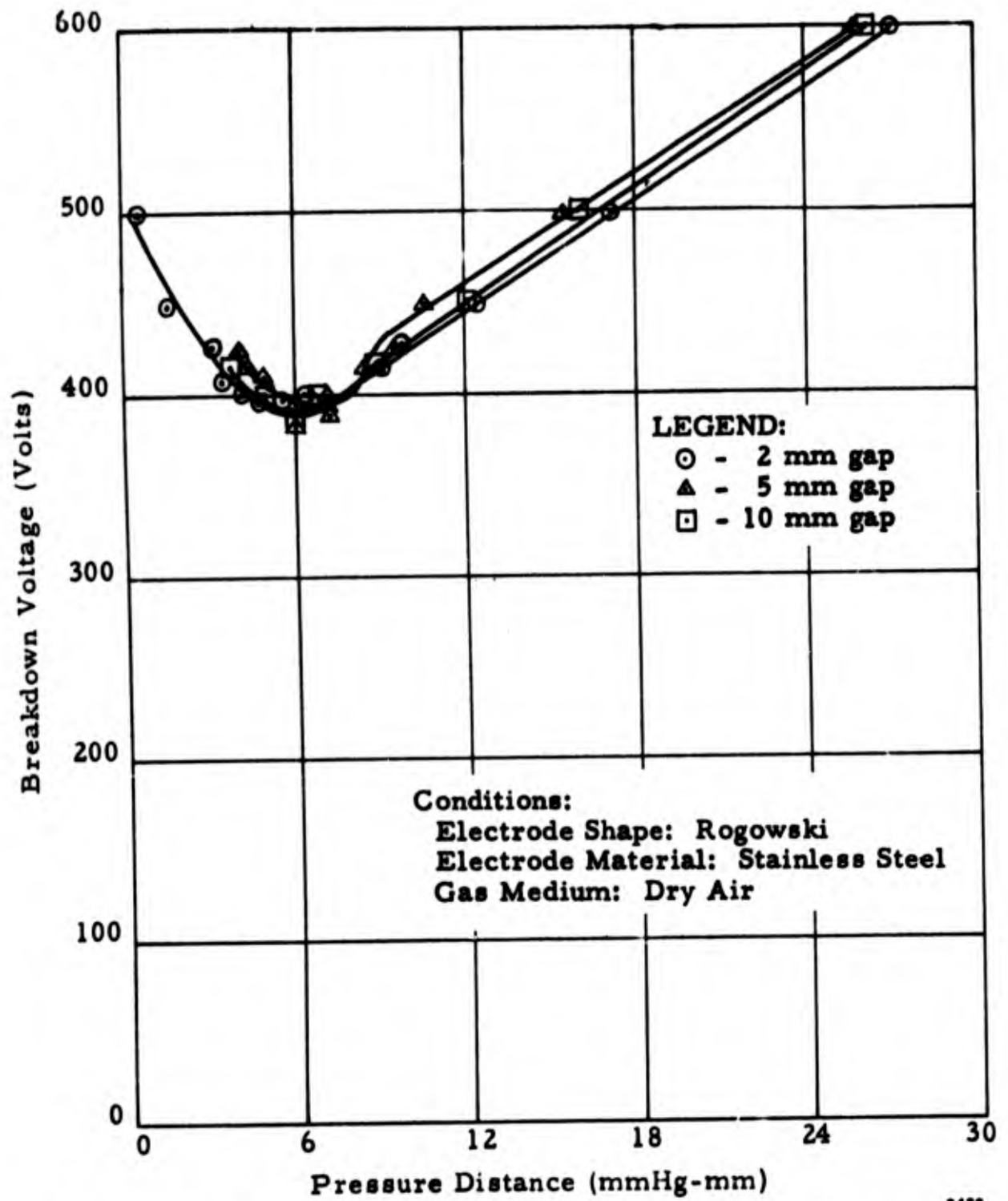


Figure 9. Short Gap Discharge Study – Comparison of Breakdown Voltages with Respect to Gap Aperture.

3428

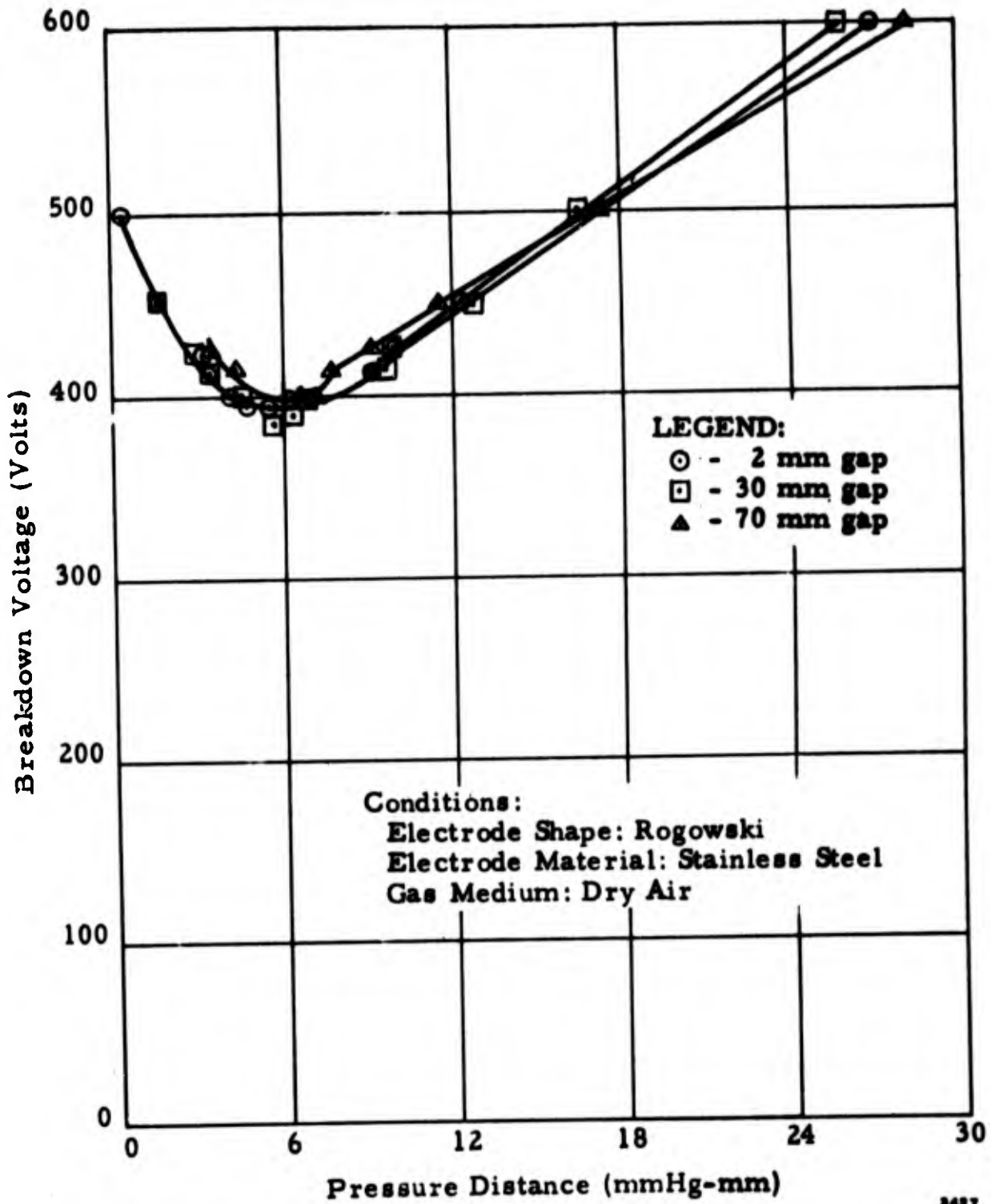


Figure 10. Short Gap Discharge Study – Comparison of Breakdown Voltages with Respect to Gap Aperture.

The value of the minimum voltage needed for spark breakdown using dry air was  $395 \pm 7.5$  volts for all spacings sampled. The minimum recorded sparking voltage was 385 volts which occurred when using the 5- and 30-mm gaps. A minimum voltage of 400 volts was required to break down the 70-mm gap. When using air having a high concentration of water vapor (approximately 95 percent relative humidity), the minimum voltage needed to produce sparking was only 335 volts. This latter magnitude closely agrees with the published values of 324 to 330 volts, obtained in tests made in areas of North America and Europe having a high average relative humidity. Ambient laboratory (approximately 40 to 60 percent relative humidity) air admitted to the vacuum chamber, caused variations of the minimum sparking voltage value by as much as 40 volts from day to day, depending upon the moisture content of the air.

The sparking curve taken for the moist air very closely follows the published sparking curves. At a pd of 30 mmHg-mm, the published sparking value is 600 volts. This agrees with the value derived from the test (see Figure 11). The use of dry air shifted the lower portion of the curve up, but it did not shift the curve laterally. Although points on the right hand portion of the curve for voltages higher than 600 were not taken, examination of the curves shows that the slope of the dry air curve is less than that of the wet air curve, indicating that the two curves would probably converge asymptotically at a higher voltage level. This will also probably occur for the left hand branch of the curve.

#### B. Pointed Electrodes

A sparking curve was also taken for the pointed terminals. The plot of this curve is shown in Figure 12. The minimum sparking voltage using dry air was 475 volts. This value occurred at 80 microns Hg or a pd product of 0.16 mmHg-mm. It should be noted that the curve is fairly level from a pd product of 6 mmHg-mm to this lower value.

The minimum voltage needed for sparking with the pointed terminals using dry air was approximately 85 volts higher than that needed to produce sparking when using the parallel plate electrodes. It was observed that some breakdowns at the lower pressures (in the micron region) set up oscillations which were indicated by a wavering ammeter needle.

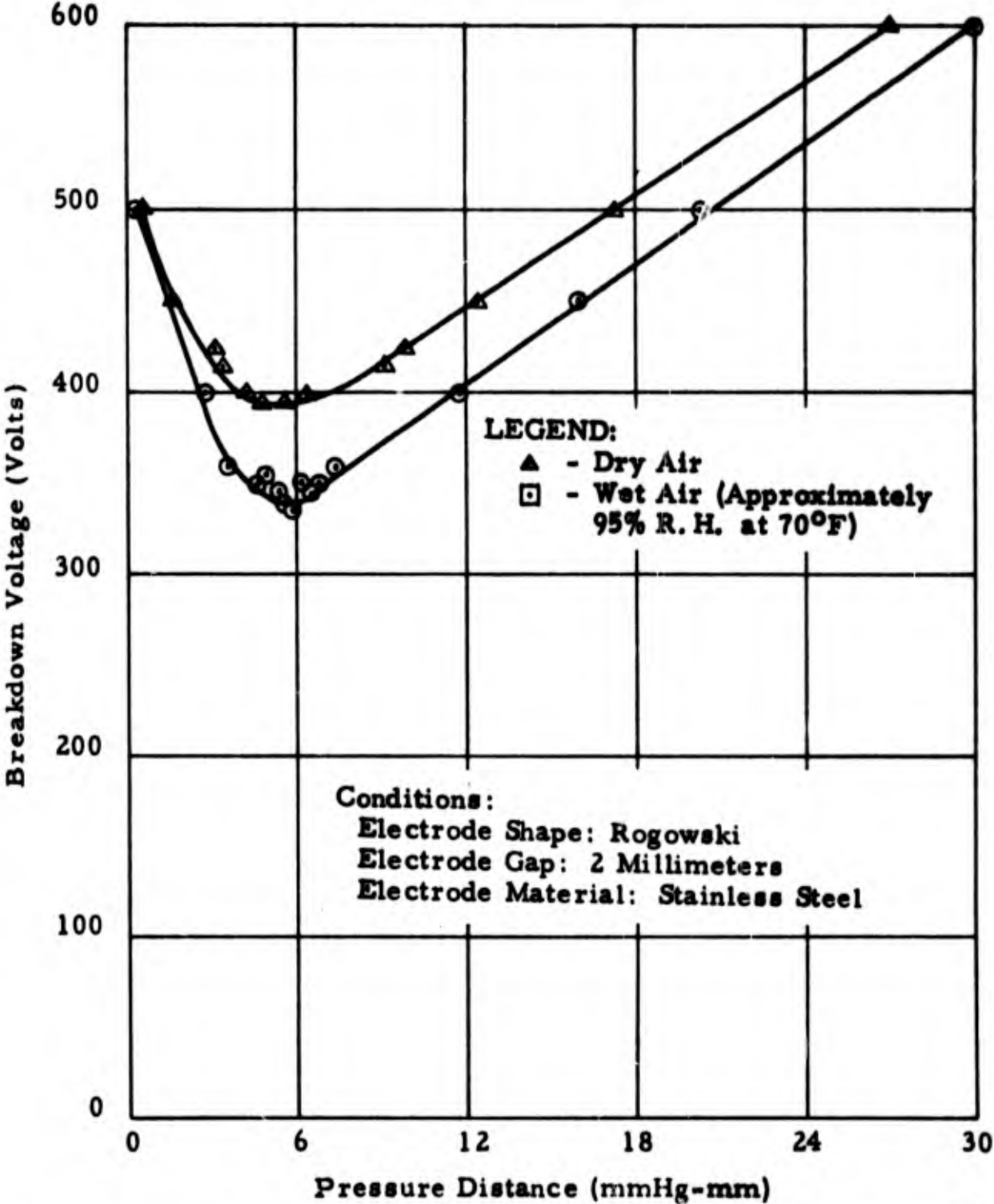


Figure 11. Short Gap Parallel Plane Discharge Study - Comparison of Breakdown Voltages.

2420

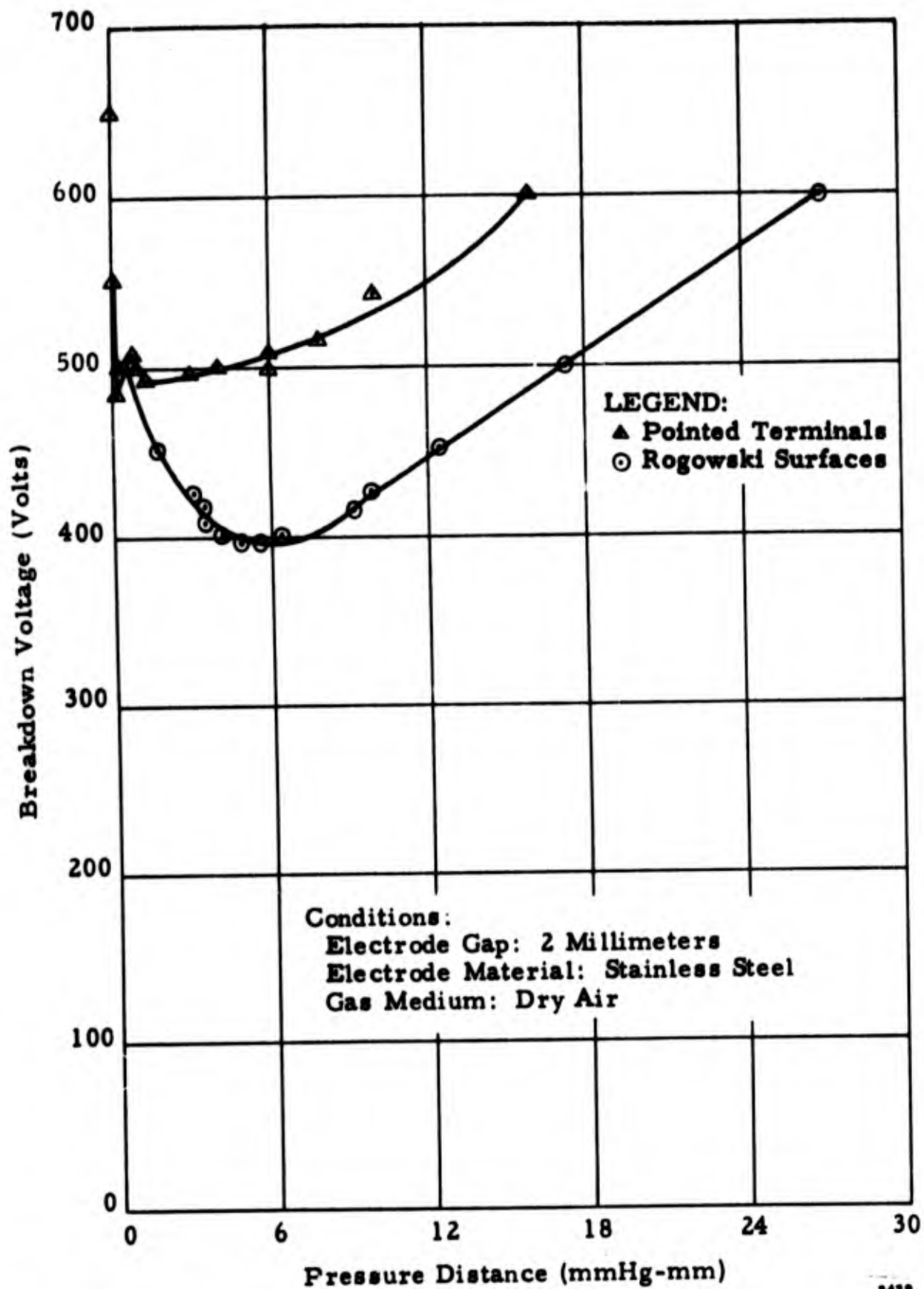


Figure 12. Short Gap Discharge Study – Comparison of Breakdown Voltages.

The minimum voltage required for sparking, using laboratory air (on a fairly damp day), was 435 volts at a pd product of 0.12 mmHg-mm.

When a glow discharge was initiated between the electrodes, the glow emanated from the surface area on the cone bounded by the tip and a circle half an inch away from the tip.

### C. Long-Gap Discharge

The minimum observed voltage for sparking noted for this portion of the testing was 675 volts (one trial out of thirty) in the pressure range of 90 to 105 microns Hg. The voltage needed for sparking was generally much higher than this — approximately 730 volts when using 120,000 ohms as the series resistance. The 675-volt value was observed when holding the pressure constant and increasing the voltage. The sparking curve is similar in shape to that taken for the parallel electrode experiments. The curve is shown in Figure 13. The minimum sparking voltage occurred at a pressure higher than that predicted by Paschen's Law. By the use of Paschen's Law (linear interpretation) and criteria for air, the breakdown should have occurred at approximately 50 microns Hg using the total short gap spacing of 122 mm. However, if half of this gap distance is used, the predicted pd magnitude and the experimentally derived value would be the same. In fact, several (a minority) of the initial breakdowns were from electrode to shell, as evidenced by one microammeter indicating a current flow while the other one did not. If the voltage was increased by as much as 5 volts, this condition ceased and both ammeters would indicate approximately the same current. However, most of the breakdowns caused simultaneous indications of current flow.

At pressures greater than 0.3 mm Hg, the initiation of the glow discharge path always seemed to be electrode-shell-electrode, which was the shorter path through the air. At pressures in the 0.1 to 0.3 mm Hg pressure range, the glow discharge path, upon initiation would be either electrode-shell-electrode (e-s-e) or electrode-electrode (e-e). In the pressure region below 0.1 mm Hg, the initiation of the glow discharge path always was e-e. The glow discharge path, after initiation at pressures below 0.3 mm Hg, would always follow the e-e path after

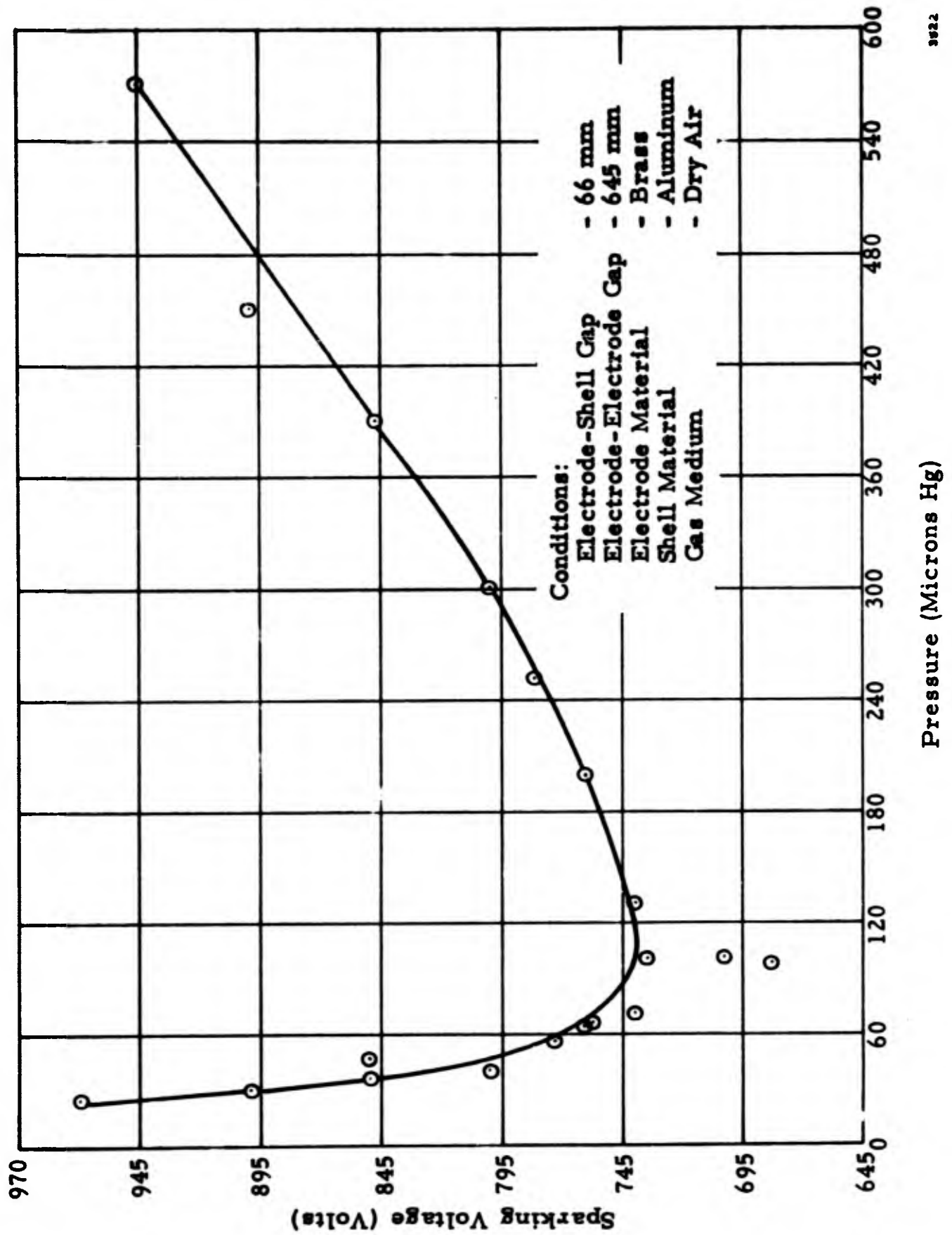


Figure 13. Long Gap Discharge - Sparking Voltage Versus Pressure.

3022

the voltage was slightly raised above the initiation magnitude. In fact, great care was taken to increase the voltage very slowly through the initiation range in order to obtain the proper initiation path. It was also noted that at the voltage just above initiation, one could obtain three dark spaces between the electrode and the shell when the discharge was e-s-e.

The test results indicated that the discharge would follow the longer of two paths when the surface of the vacuum vessel was a conducting medium. Many tests which have been accomplished in the past to demonstrate this phenomenon used glass, a nonconducting medium, as the vacuum container. Thus, the use of a conducting shell did not invalidate the prediction that a discharge could follow the longer of two paths if the pressure were reduced below some given value.

The curves depicting the volt-ampere characteristics of the gap are found in Figures 14 through 20.

Examination of the plot of "Gap Voltage Versus Applied Voltage" indicates that the slope of the gap voltage decreases as the series resistance is increased and finally becomes negative for a resistance value of 2 megohms. This indicates that the resistance of the gap decreases with an increase in actual applied voltage. The curves showing the percentage of power dissipated in the gap (Figures 16 and 18) indicate that the percentage of total power dissipated in the gap decreases with an increase in applied voltage for a given series resistor value. Examination of the curves in Figures 15 and 16 indicates that no data were taken for an applied voltage of 700 and 750 volts for the 2 megohm resistance value. This is true because these gap voltages dropped below the extinction voltage. As the resistance was increased, the value of the sparking voltage required also increased. This is further proof of the claims of Rogowski and others that the value of sparking voltage depends on the magnitude of the saturation current which again is dependent on the impedance in series with the gap and the voltage sources.

## VIII. DISCUSSION AND RECOMMENDATIONS

Study of the literature, as mentioned in Section III, and the exacting care needed during the testing period to obtain consistent data, indicates that only a few of the variables affecting sparking can be accounted for by mathematics when a

**BLANK PAGE**

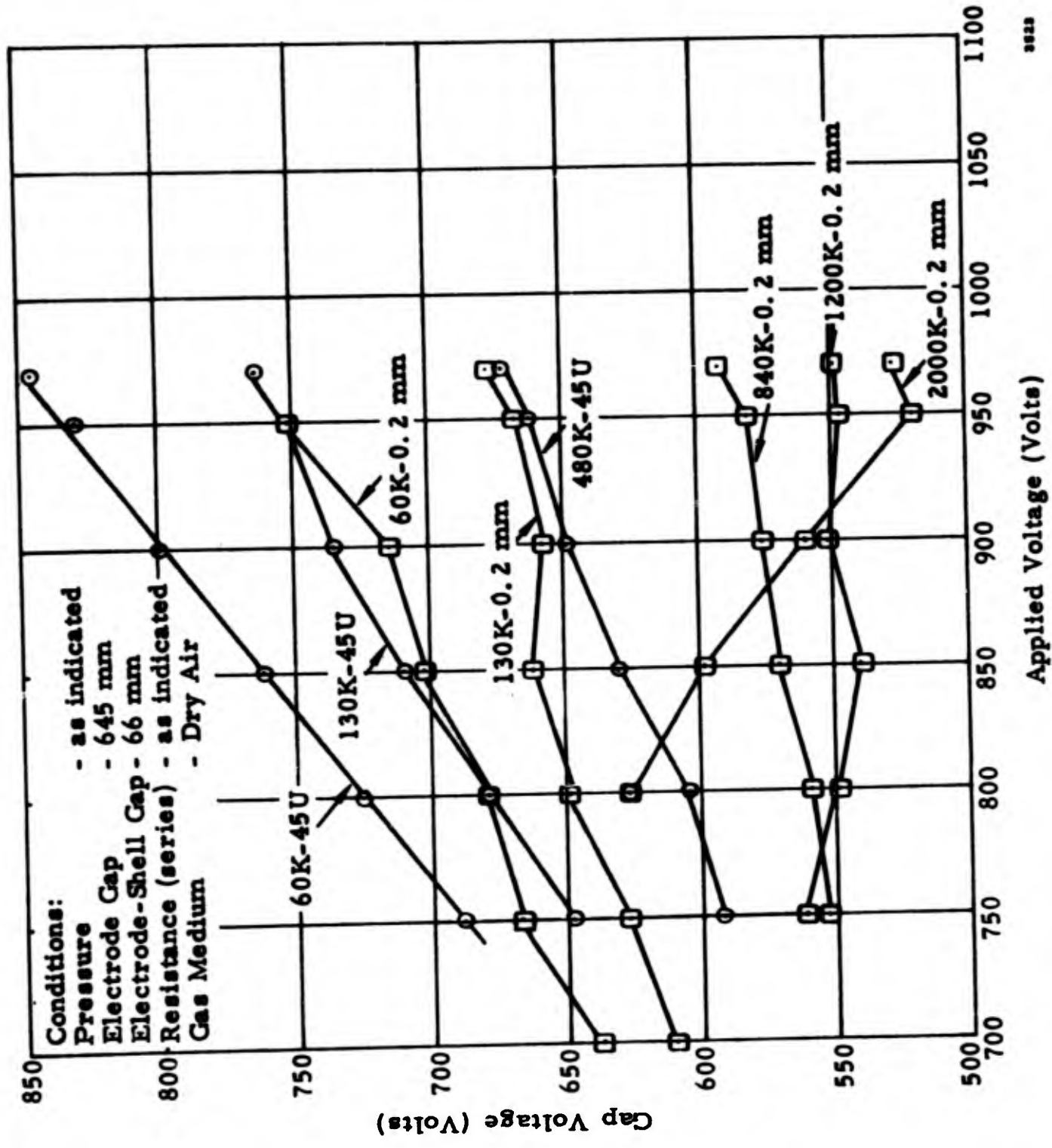


Figure 14. Long Gap Discharge - Gap Voltage Versus Applied Voltage.

25

1/2  
**FRAMES**

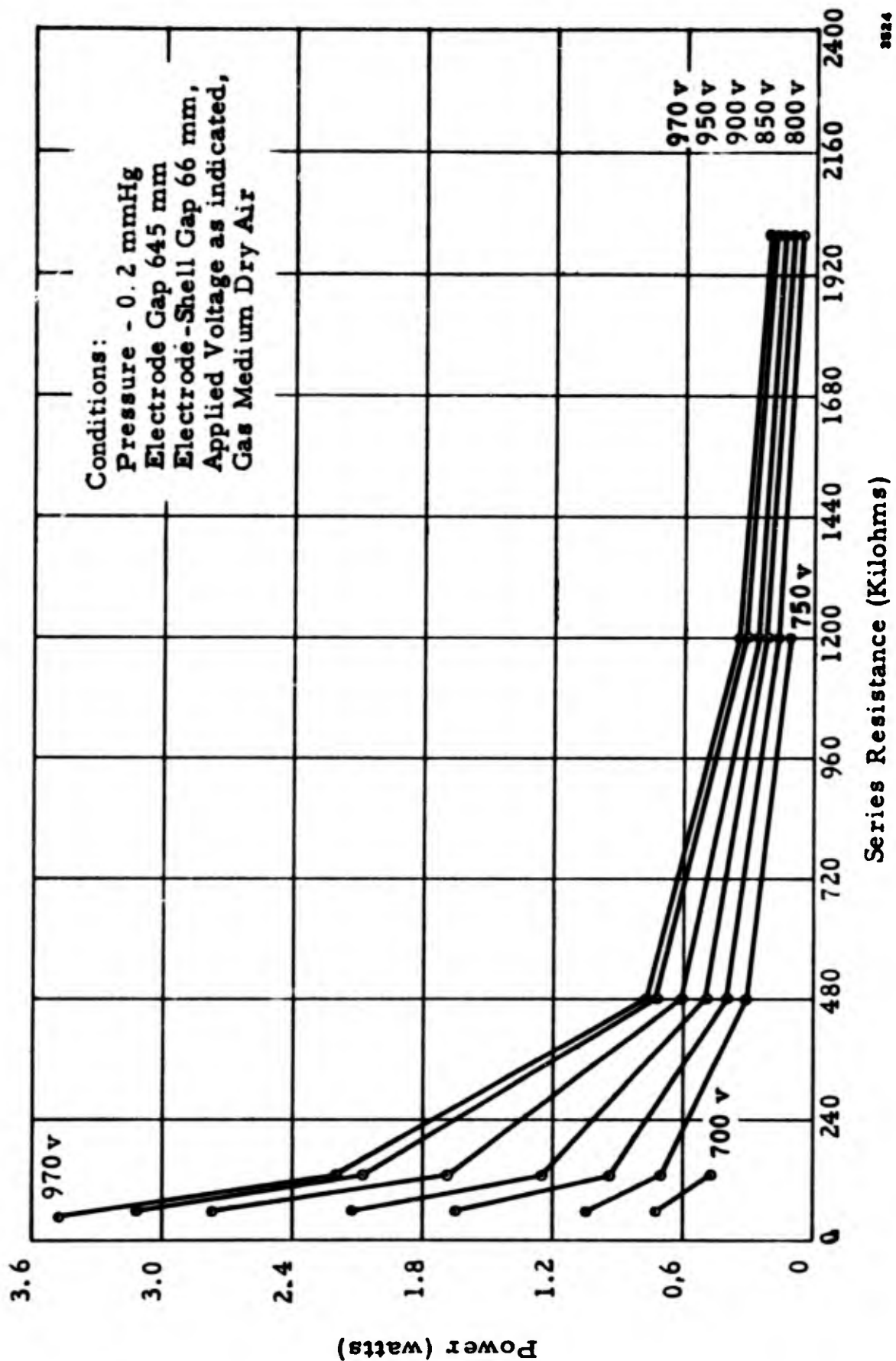


Figure 15. Long Gap Discharge - Total Power into Circuit.

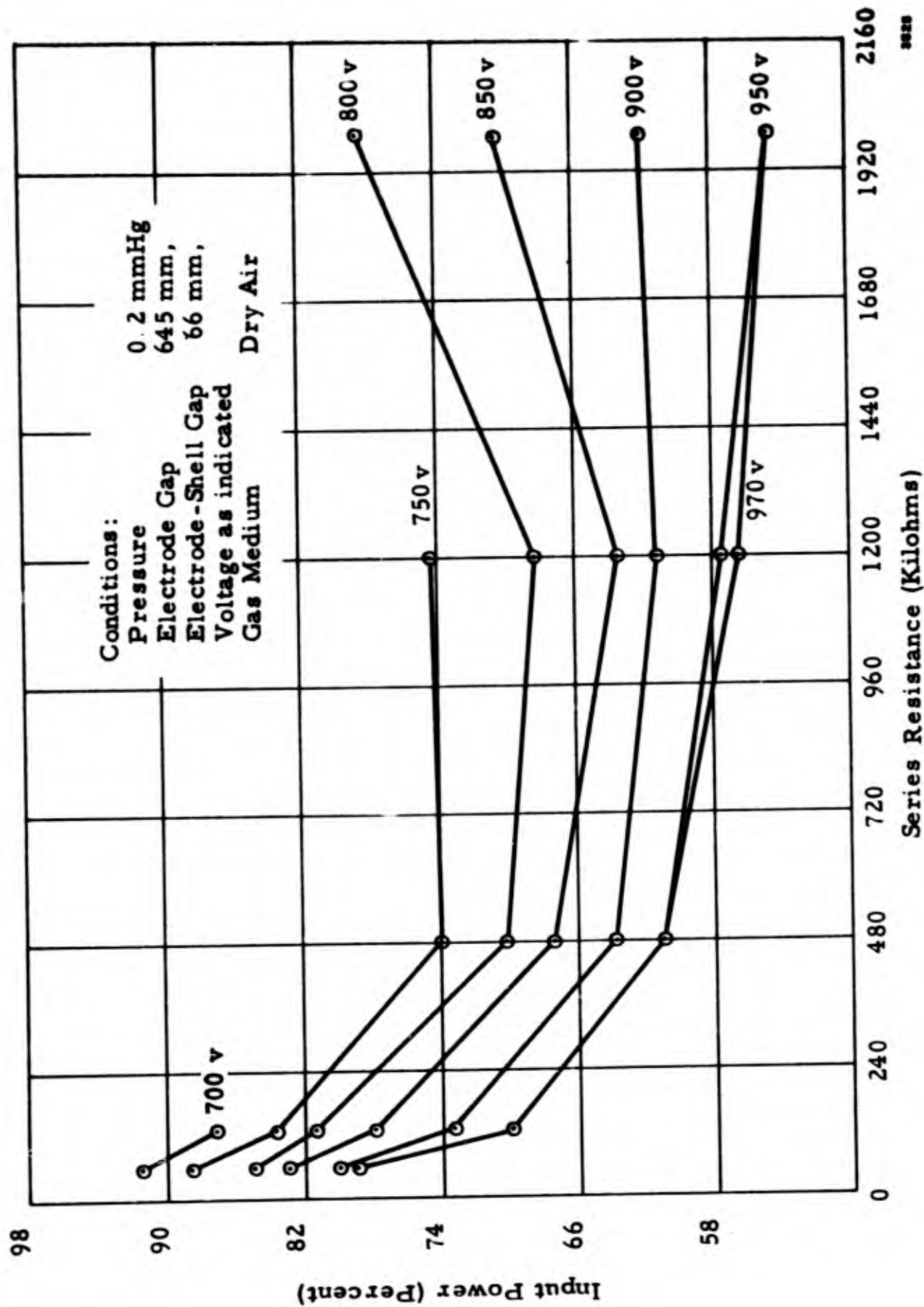


Figure 16. Long Gap Discharge - Percentage of Power Input Dissipated in the Gap.

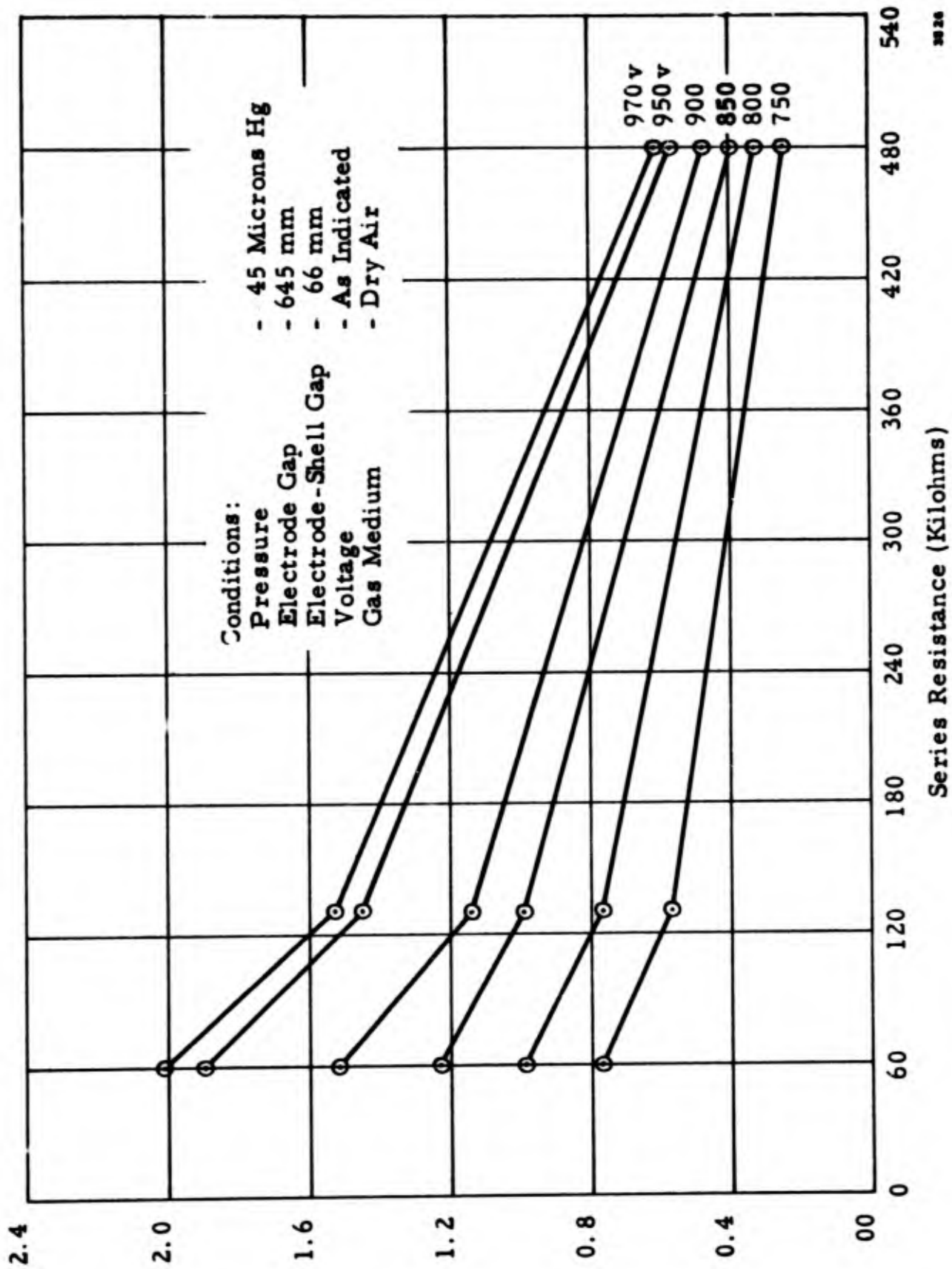


Figure 17. Long Gap Discharge - Total Power into Circuit.

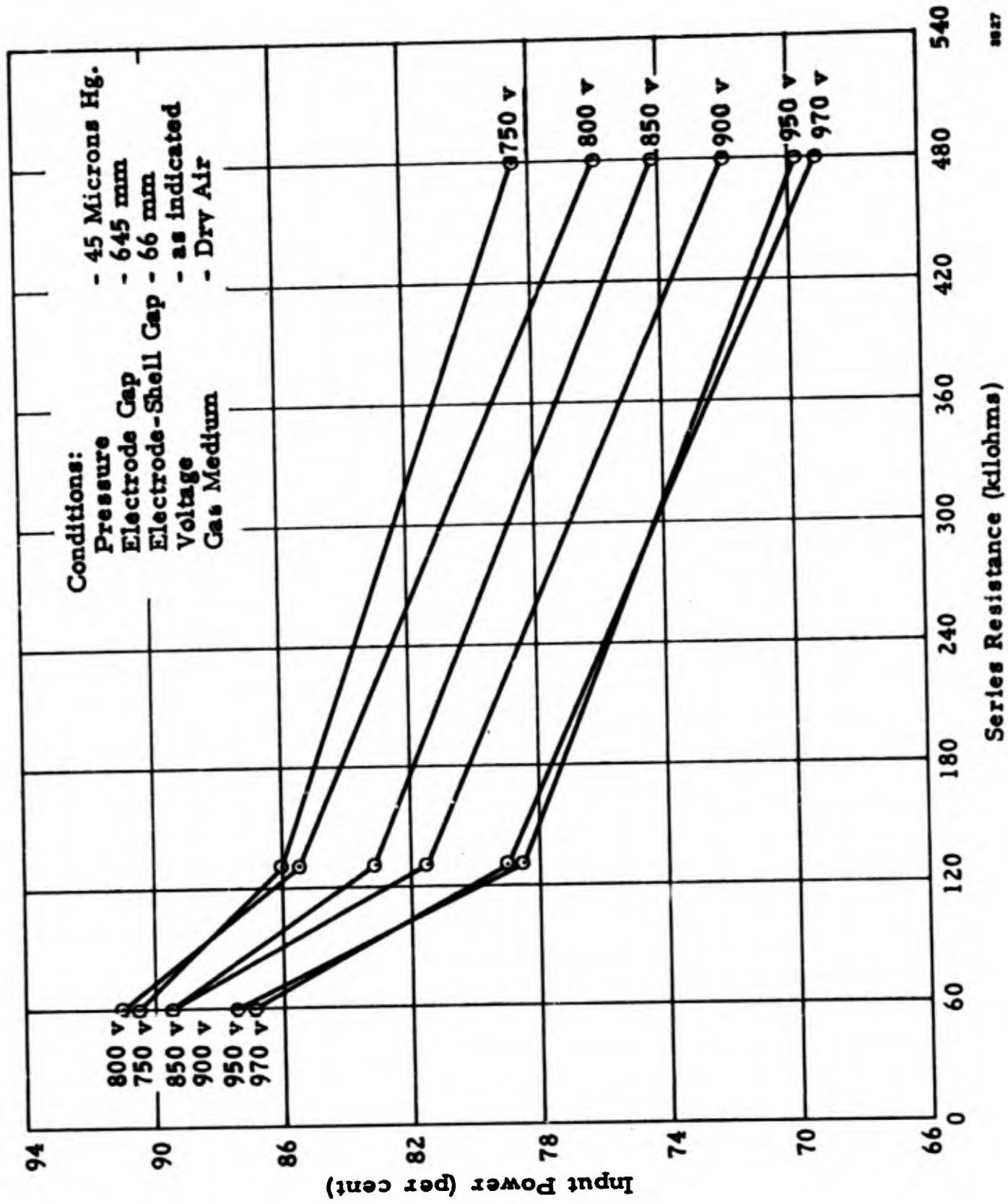


Figure 18. Long Gap Discharge - Percentage of Power Input Dissipated in the Gap.

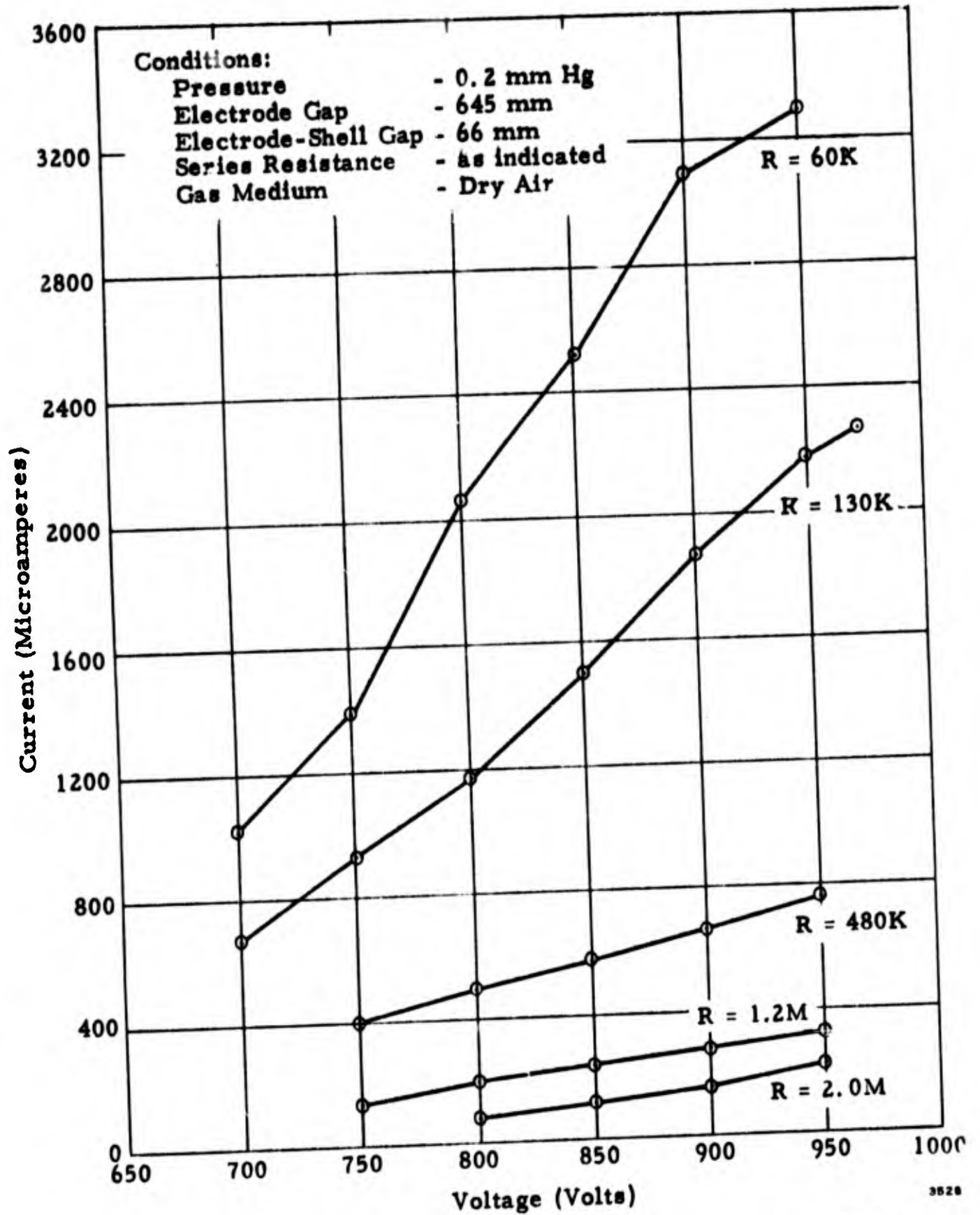


Figure 19. Long Gap Discharge - Current Versus Applied Voltage.

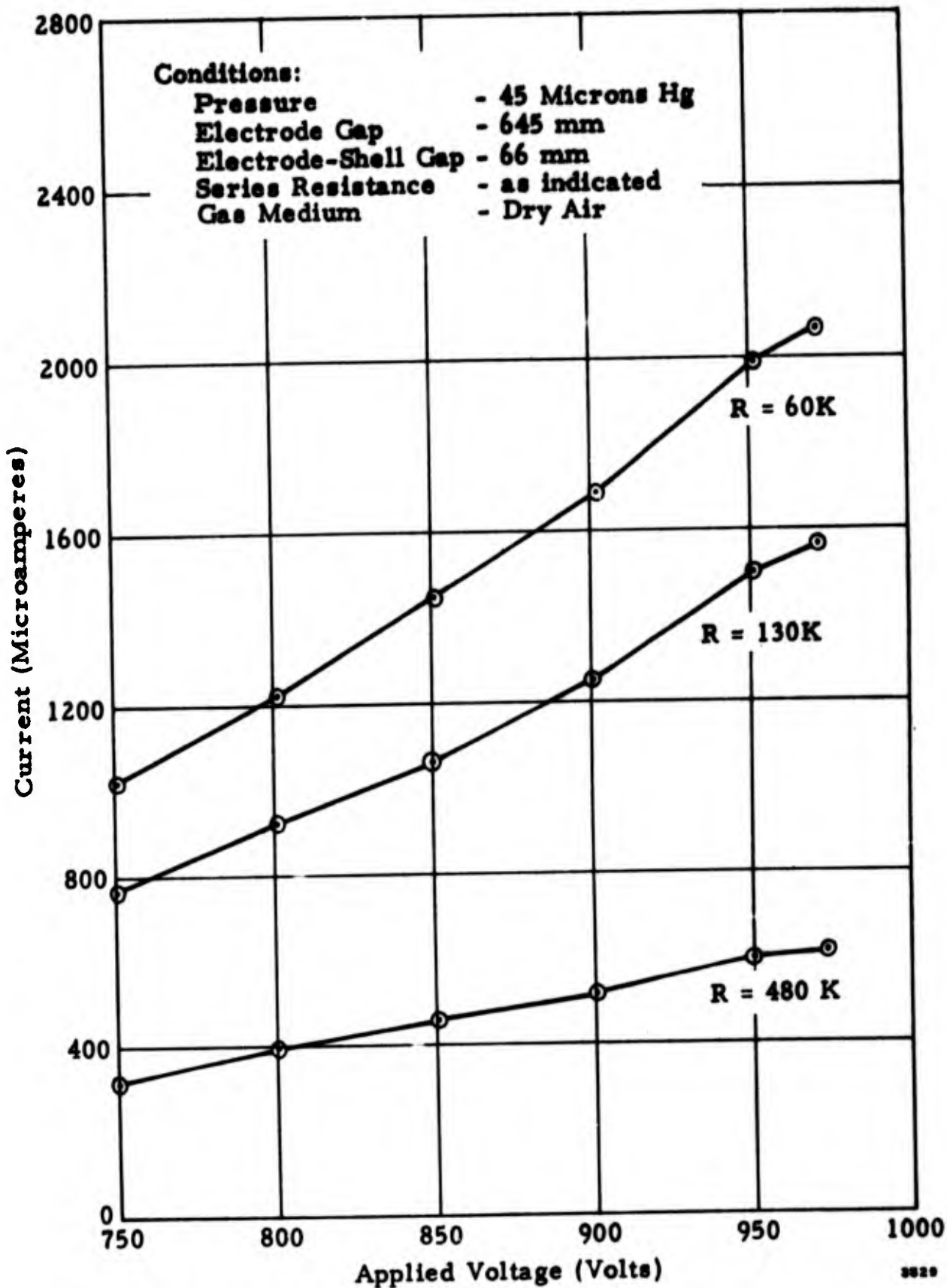


Figure 20. Long Gap Discharge - Current Versus Applied Voltage.

"black box" with uninsulated wiring is considered. Even some of the earlier experimentally found values of sparking voltages are now considered invalid for some gases because the experimenters had contaminated their gas medium with mercury. It is therefore imperative that the specimen, if it is to operate at high altitudes, have its operation checked while it is subjected to altitude tests in a laboratory. This is particularly true if the voltage used exceeds the value of 200 volts as recommended in Appendix I. This value was derived from the use of the cathode fall voltage for lead, which is a component of solder. This value may be somewhat on the "safe" side because of the following information: the minimum sparking voltage encountered in a previous STL experiment using solder-covered bolt heads as terminals was found to be higher than that needed for the breakdown of the parallel-plane gap. The Convair experiment using wiring soldered into the MS connectors also showed a minimum sparking voltage of 365 volts.

The sequence of testing is also important. Since the presence of water vapor lowers the voltage needed to initiate sparking, the altitude test should follow within a specified short time period after the specimen has been subjected to humidity testing. Since many of the airborne electronics black boxes are potted, vibration should also be applied prior to the altitude testing. This will check the potting material and process because any openings in the potting will most likely cause a lower sparking voltage than that which may be anticipated using air as the sole means of insulation. The reasons for this lowering of the sparking voltage have already been discussed in Section III.

Examination of the literature indicates that when a wire is negative with respect to a coaxial cylinder, the minimum sparking voltage is less than that required when the wire is the positive electrode (370 versus 500 volts). This leads to the recommendation that all powered uninsulated wiring should be kept positive with respect to the surrounding metal structure.

If a corona breakdown occurs in a missile component aboard a missile, it may not only cause failure of the unit within which it occurred, but it may also cause a malfunction elsewhere because of radiation of energy at r-f frequencies. It was noted during the testing at STL that at voltages greater than the minimum

sparking voltage (i. e., in the left-hand branch of the sparking curve) and at a pd product less than that needed for this minimum sparking voltage, corona did occur. The voltage at which this occurred was lower than the sparking voltage predicted for that pd product. This corona contained pulses of 1 to 5 milliseconds duration. These pulses contained frequency components in the 1 megacycle range. No corona occurred at voltages less than the minimum sparking potential. The minimum initiation voltage necessary to produce corona, as recorded in Convair's experiment, is equivalent to some of the minimum magnitudes derived from the STL testing when ambient air was pumped into the system. The 365-volt figure also corroborates the 370 volts indicated by Meek and Craggs (Reference 15, p. 120).

The pressure region in which the minimum sparking potential can occur can be predicted by the use of Paschen's Law for some of the geometrical configurations used aboard missiles. Thus, if one states that the product of pd is 6 mmHg-mm spacing, then if d is known, p can be calculated. In the Convair tests (Reference 21), the distance between pins on the MS connectors tested was approximately 3 to 5 millimeters. Calculations show that the minimum sparking voltages should be in the pressure range of 2 mm Hg to 1.2 mm Hg. The minimum sparking voltage did lie in this range. Thus, the altitude sparking voltage can be approximately predicted (care should be exercised when using this calculation because a highly distorted field invalidates it). If the testing equipment is adequate to attain this altitude, then the operation of the electrical specimen should be checked at this altitude.

The foregoing discussion does not pertain directly to sparking at frequencies higher than 1000 cps, especially r-f and higher frequencies. Information upon this subject may be found by consulting some of the references presented in the Bibliography (References 1, 2, 3, 6, 9, 12, 13, 15, 16, 19, 20, 23, 24 and 28).

A word of caution should be added about the testing of any specimen for sparking in an altitude chamber. Sparking may not occur in the chamber, but yet occur in the missile installation. This is due to the fact that free electrons may be available in the missile environment but they might not be available in the test chamber. To decrease the possibility of the event occurring in one

environment and not in the other, a radioactive source such as polonium should be placed next to the specimen in the test chamber. This will increase the probability of electrons entering a critical gap area, thus increasing the probability of breakdown. Polonium has been suggested because its use is not so restricted or dangerous as that of other radioactive sources such as Cobalt 60 (Reference 3).

Note should also be taken of the fact that the conditions used for testing of voltage breakdown in ballistic missile components should differ from those used for similar testing of components for space applications. Testing for voltage breakdown in space conditions must take account of expected radiation and temperature parameters, which also influence such breakdowns to a very important extent.

This study has indicated under what conditions sparking may be expected under low pressure conditions. A word should be added about possible means of preventing such sparking in ballistic missiles or space applications.

The first preventive measure, which has already been mentioned, is to keep the voltage differential between adjacent exposed conductors below 200 volts. This figure is used rather than the 300 volts indicated by the study in order to provide a safety factor against possible surface flashover. In this connection it is important to check for the maximum possible instantaneous voltage differentials which might exist between the conductors in question. For example, the maximum voltage differential between a 200 volt d-c conductor and a 208 volt rms a-c current is not 8 volts or 91 volts, but 491 volts, requiring considerably more attention to the voltage breakdown problem than would appear from the given voltages. \*

A second method for prevention of arcing is the encapsulation or potting of all susceptible conductors, including tube bases. One method used for potting of tube bases which preserves the original ease of removal and replacement is the application of a silicon grease in a layer at least one eighth inch thick to the base of the tube (Reference 30). Care must be taken, as noted earlier, that in applying

---

\* See Appendix I, Section G.

the grease one leaves no fissures which will provide possible surface flashover path at lower voltages. This method should be a temporary fix because the fissures will occur if the tubes are changed without reapplying a coat of grease or if the grease is allowed to stand long periods of time before the item is used. It is also important in connection with potted connectors to be sure that the connector is designed for high-altitude use. In other connectors voltage breakdown at high altitudes will occur at the interface of the two halves of the connector, even though the wiring on the back side of the connector is adequately potted.

A third possibility for prevention of voltage breakdown, in case it is not possible or desirable to keep the voltage low enough or to encapsulate or pot the conductors, is to pressurize the entire unit so that the environment is kept at a simulated low altitude. This method is effective but cumbersome for fabrication, assembly, and checkout, and suffers from the additional drawback for space applications that the pressurized unit may be expected eventually to leak, thus reducing the internal pressure to a value where voltage breakdown will occur if the high voltage equipment is in an operating state.

Where insulators are used in a cavity type unit, it is important that all parts, after thorough cleaning, be handled with clean nylon gloves. If this precaution is not taken there is danger of electrical breakdown through the grease remaining on the surface of the conductor or insulator from the handling process. The minimum sparking voltage in such units can be raised through the use of conducting materials which have been cast in a vacuum.

A final method of preventing voltage breakdown in space vehicles can be inferred from an examination of the curves representing Paschen's Law. The curves predict that as the pressure is reduced below that required for the minimum sparking voltage, the voltage necessary for sparking must increase again. Thus if high voltages are required in a space vehicle the sparking problem can be avoided by keeping these items in an "off" condition until the vehicle has passed through the dangerous zone of altitude into one where the pressure is so low that the sparking voltage is above the value used in the equipment. The high-voltage current can then safely be turned on by command, by timer, or by pressure sensor.

## APPENDIX I

A. Electric Current in Gases (Reference 26, pp. 1-10)

The first report that gases were able to conduct electricity was made in 1785 by Coulomb, who concluded that the loss of charge from a gold-leaf electroscope could not be entirely accounted for by the electrical leakage through the insulation. In 1900, Wilson and Geitel independently reported experiments which gave proof of electrical conduction by gases. In Wilson's experiments, the apparatus was designed so that electrical leakage across an insulator would maintain the charge on an electroscope, instead of allowing its discharge. However, the electroscope became discharged, and the only possible leakage path was through the air, so that direct proof was obtained for Coulomb's theory.

In the following work it was found that gases do not obey Ohm's Law. With a potential difference applied between two electrodes in a gas, the electric current through the gas does not increase linearly as the voltage is increased. (See Figure I-1.) With a continued increase of voltage, the current rises to a constant value, then increases first slowly and then more and more rapidly, until finally a spark discharge occurs.

It was also found that the conductivity of a gas could be increased tremendously by subjecting it to radioactive material, X-rays, ultraviolet light, or a flame, and that the increased conductivity was due to ionization of the gas. The small natural conductivity of the gas without the presence of the strong ionizing agent was determined to be due to ions formed by cosmic radiation and to the small amount of radioactive material present everywhere.

If all of the ions formed between two electrodes by a constant ionizing source are drawn to the electrodes before they can recombine, the current in the gas is constant and is called saturation current. In a chamber of fixed volume, as an ionization chamber, the saturation current  $i_0$ , is given by

$$i_0 = quU \quad (1)$$

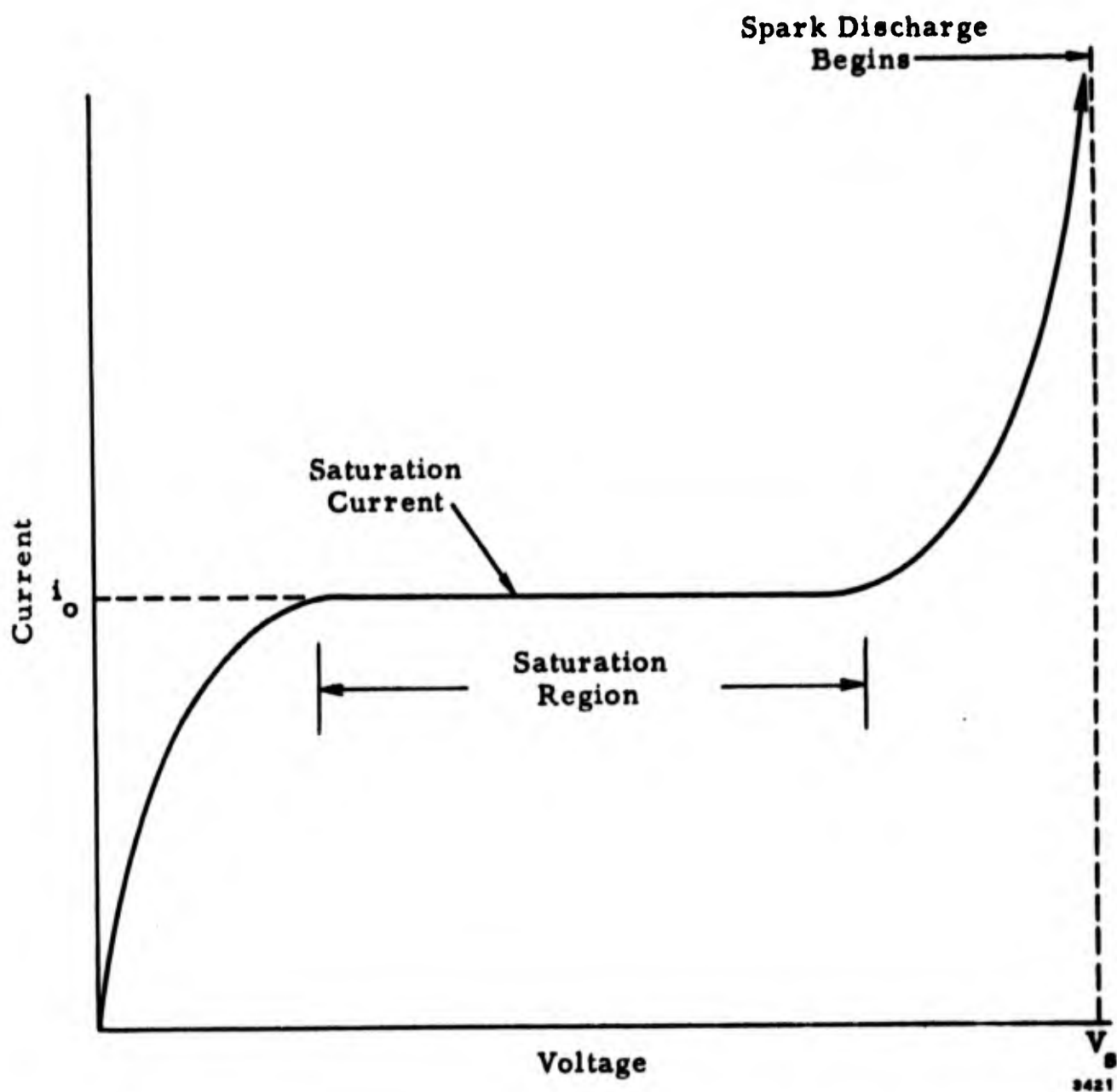


Figure I-1. Current in an Ionization Chamber with Increasing Voltage.

where

- $q$  = number of new ion pairs formed per unit volume per second,  
 $e$  = average electric charge per ion,  
 $U$  = volume of chamber.

B. Townsend's Equation (Reference 26, pp. 11-27; Reference 15, pp. 67 and 68.)

Townsend's work in explaining the increase of current with voltage after saturation and up to the initiation of the spark discharge is definitive and still stands unchallenged in its essential details. He theorized that the movement of ions in the saturation region was too slow to cause new ionization when the old ions collided with nonionized particles. However, as the voltage was increased, the increase of electric field strength caused greater acceleration to those ions already present. Eventually, the voltage was increased until some ions attained velocities such that ionizing collisions began to occur, and the total current then increased because of the additional new ions being formed.

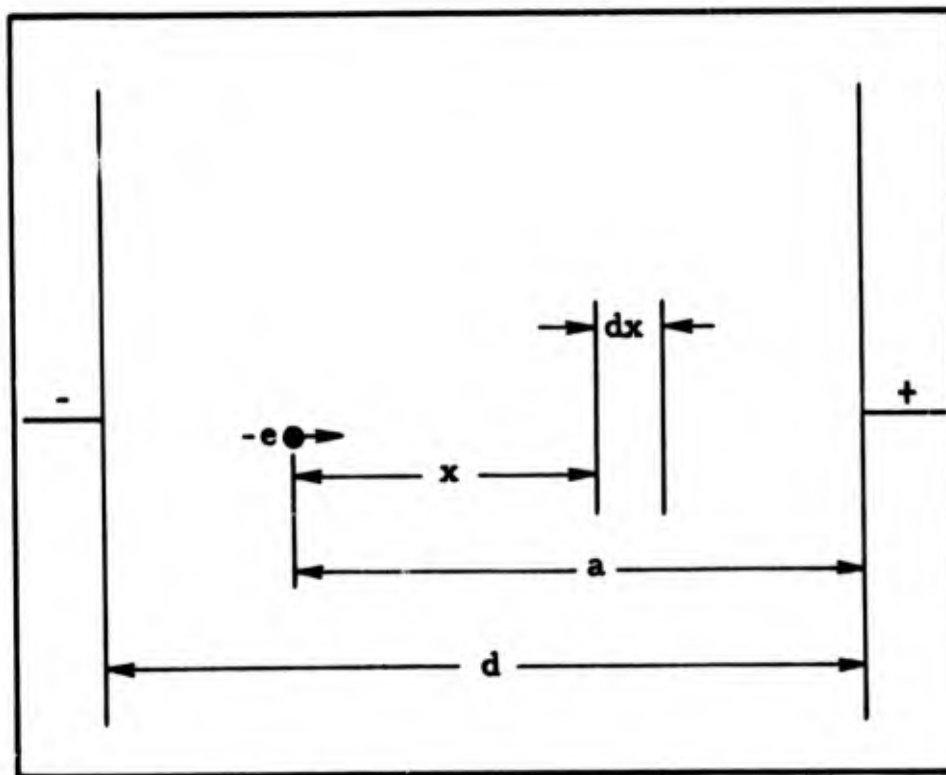
The primary cause of the increased ionization in the strong electric field was determined to be collision of negative ions with nonionized molecules of gas, and the collisions in the gas due to positive ions were found to be of secondary importance. (Most of the negative ions are known to be electrons; for the sake of simplicity, this discussion will consider all negative ions to be electrons.) However, the study of Townsend and others gave consideration to the formation of new ions by several means other than merely collisions between ions and nonionized molecules in the gas. Bombardment of the cathode by positive ions was also found to cause emission of electrons. Photoelectric emission of electrons from the cathode due to radiation from excited atoms in the gas was another possible contribution to ion formation.

The complete mechanism of the increased ionization current in the strong electric field is very complicated. It turns out that it is necessary to consider only the new ion pairs formed by electron collision with nonionized atoms, and the electron-emission from the cathode by positive ion bombardment. Other mechanisms contribute only a trivial part of the ionization current, and their contribution is now generally lumped into the positive ion bombardment.

Consider first the ionization produced by collision of free electrons with gas molecules. In the passage of an electron from its point of inception to the anode, it may form many additional ion pairs, an avalanche. The number of additional ions formed depends upon the product of the mean free path of the electrons and the electric field strength; the distance traveled between collisions must be sufficient for the electrons to have time to acquire ionizing velocity, or the electric field must be great enough to give this velocity in a short space. This is treated more thoroughly in Section C of this Appendix.

Suppose one free electron travels a total distance  $a$  to the anode (Figure I-2). Let  $\alpha$  be the number of new pairs of ions formed by collision per unit distance of travel by an existing free electron. Let  $n$  be the number of ions existing due to the one original free electron after it has traveled a distance  $x$ ;  $n$  includes the original electron. Within a small additional distance  $dx$ , let the total number of new ion pairs formed be  $dn$ . The number of new ions formed by a single existing free electron is  $\alpha dx$ , so that the number of ions formed by  $n$  existing free electrons is

$$dn = n \alpha dx . \tag{2}$$



3422

Figure I-2. Ionization by Collision.

The number of ions,  $\underline{n}$ , increases from 1 to  $\underline{n}_a$  while the original free electron travels from  $x = 0$  to  $x = a$ . Therefore, separating variables, and integrating over these limits

$$\underline{n}_a = \epsilon^{aa} . \quad (3)$$

That is, for every electron starting at a distance  $\underline{a}$  from the anode, the number of ions reaching the anode is  $\underline{\epsilon^{aa}}$ .

Let us assume that most of the original electrons are emitted from the cathode by any reasonable mechanism, and that this amounts to  $\underline{N}_o$  electrons per second per unit area of cathode. The distance traveled is  $\underline{d}$ , from cathode to anode, and the total number of ions arriving at the anode per second per unit area is given by Equation (3) as

$$N = N_o \epsilon^{ad} . \quad (4)$$

If the charge carried by each ion is  $\underline{e}$ , the current density is, from Equation (4),

$$i = Ne = N_o e \epsilon^{ad} = i_o \epsilon^{ad} ; \quad (5)$$

$\underline{i}_o$  is the saturation current of Equation (1) in terms of current density, provided that only a negligible quantity of negative ions originate elsewhere than the cathode.

The expression of Equation (5) accounts for the current due to the ions being formed by the original electrons. For each of the original ions, Equation (3) shows that  $\underline{\epsilon^{ad}}$  electrons reach the anode. This means that  $\underline{(\epsilon^{ad} - 1)}$  ion pairs are formed in the gas for every original electron. Then, if  $\underline{N_o \epsilon^{ad}}$  ions begin at the cathode,  $\underline{N_o (\epsilon^{ad} - 1)}$  ion pairs were formed in the gas. But this means that  $\underline{N_o (\epsilon^{ad} - 1)}$  positive ions reach the cathode, and may cause additional electrons to be emitted from the cathode. Suppose that for each of the positive ions reaching the cathode, a fractional quantity,  $\underline{\gamma}$  of electrons is emitted. The number of new electrons generated by the positive ions is then  $\underline{\gamma N_o (\epsilon^{ad} - 1)}$ .

But, for each one of these new electrons, we have again  $\epsilon^{\text{ad}}$  ions reaching the anode, so that  $\gamma N_0 (\epsilon^{\text{ad}} - 1) \epsilon^{\text{ad}}$  negative ions reach the anode in all. The new positive ions formed are again given by  $(\epsilon^{\text{ad}} - 1)$  for every electron beginning the journey. Hence, there are an additional  $\gamma N_0 (\epsilon^{\text{ad}} - 1)(\epsilon^{\text{ad}} - 1)$  positive ions reaching the cathode, and each of these causes the formation of another  $\gamma$  electron, or  $\gamma^2 N_0 (\epsilon^{\text{ad}} - 1)(\epsilon^{\text{ad}} - 1)$  more electrons.

Briefly, the process described shows how each of the original electrons may create new ions, such that each of the new ions has a probability of creating additional ions. The sum of all of the ions produced per unit time is a finite number. If we sum up all the electrons arriving at the anode per second per unit area, we have, according to the process described,

$$\begin{aligned} N &= N_0 \epsilon^{\text{ad}} + \gamma N_0 (\epsilon^{\text{ad}} - 1) \epsilon^{\text{ad}} + \gamma^2 N_0 (\epsilon^{\text{ad}} - 1)^2 \epsilon^{\text{ad}} + \dots \\ &= N_0 \epsilon^{\text{ad}} [1 + \gamma (\epsilon^{\text{ad}} - 1) + \gamma^2 (\epsilon^{\text{ad}} - 1)^2 + \dots] \\ &= N_0 \epsilon^{\text{ad}} \frac{1}{1 - \gamma (\epsilon^{\text{ad}} - 1)} \end{aligned}$$

The current density is given by

$$i = Ne = N_0 e \epsilon^{\text{ad}} \frac{1}{1 - \gamma (\epsilon^{\text{ad}} - 1)}$$

or

$$i = \frac{i_0 \epsilon^{\text{ad}}}{1 - \gamma (\epsilon^{\text{ad}} - 1)} \quad (6)$$

This is the form of Townsend's equation which is most nearly supported by physical theory.

It should be noted that  $\gamma$  is a function of electric field strength and gas pressure, as is  $\alpha$ . In the region of the saturation current (Figure I-1),  $\gamma$  approaches zero, and Equation (6) reduces to Equation (5). Equation (5) was deduced on the basis of the original electrons being emitted from the cathode. If this condition does not obtain, e. g., if most of the original ions originate in the gas, then Equation (5) is no longer valid, and another expression should be used. However, this affects Townsend's equation only in the value of saturation current used, which must be measured empirically in any actual experiment. In the voltage region above saturation leading to sparking, the original ionization process is soon overshadowed by cathode emission due to positive ion bombardment. It will be seen in the following that the saturation current is not a factor in establishing the sparking voltage.

C. Townsend's Criterion for Sparking (Reference 26, pp. 25 and 26; Reference 15, p. 80.)

Townsend's equation, Equation (6), determines the conditions necessary to initiate a spark discharge, and then leads to Paschen's Law. (The spark discharge may be simply defined as an electric current in a gas self-sustained by electron emission from the cathode due to positive ion bombardment, with given conditions of pressure, voltage difference, and electrode configuration.) Referring again to Figure I-1, it may be seen that the current increases ever more rapidly with voltage increases above the saturation region. The current density actually increases by a factor of  $10^6$  or more when the electrical breakdown of the gas occurs, and is limited only by the circuit impedance and by ionization of nearly all the available gaseous atoms. Mathematically, we may assume that the ionization current becomes infinite, and then investigate the means of causing this increase.

It is evident that the numerator of Equation (6) cannot account for the current increase,  $i_0$ ,  $\alpha$ , and  $d$  all being finite variables. However, if the denominator approaches zero, then the total current increases without bound, all other things remaining as before. Therefore, Townsend's criterion for sparking is that the denominator vanishes,

$$1 - \gamma (\epsilon^{\alpha d} - 1) = 0 \quad (7)$$

or

$$\gamma(\epsilon^{\text{ad}} - 1) = 1.$$

Generally, the number of ion pairs  $(\epsilon^{\text{ad}} - 1)$  produced by one original ion is much greater than one, so that we may use

$$\epsilon^{\text{ad}} \approx \epsilon^{\text{ad}} - 1.$$

Then, from Equation (7), we have the approximate form of Townsend's sparking criterion,

$$\gamma\epsilon^{\text{ad}} = 1. \quad (8)$$

For clarity, the symbols are redefined:

- a, the first Townsend coefficient, is the number of new pairs of ions formed by collision per unit distance of travel by an existing free electron.
- y, the second Townsend coefficient, is the average quantity of electrons emitted from the cathode for each positive ion bombarding the cathode. (Other minor secondary sources are lumped into y.)
- d, the distance between the electrodes.

This may be interpreted as follows (cf. Reference 15, p. 80):

- a. For  $\gamma\epsilon^{\text{ad}} < 1$ , the discharge current i is given by Equation (6), and is not self-maintained; i. e., if the primary source of ions providing the saturation current i<sub>o</sub> is removed, the current i will cease.
- b. For  $\gamma\epsilon^{\text{ad}} = 1$ , the number ε<sup>ad</sup> of ion pairs produced by one electron avalanche is sufficiently large that the resultant positive ions from that avalanche are able to cause emission at the cathode of one additional electron, on the average. The discharge is then self-maintaining in the absence of the original source producing the saturation current i<sub>o</sub>, so that  $\gamma\epsilon^{\text{ad}} = 1$  defines the sparking threshold.

c. For  $\gamma e^{ad} > 1$ , the ionization produced is cumulative, and the final limitation on the current is due only to the nearly complete ionization of the gas, the mobility of the ions, and the exterior circuit impedance. As stated previously, both Townsend coefficients  $\underline{\alpha}$  and  $\underline{\gamma}$  are functions of the electric field strength,  $\underline{E}$ , and the gas pressure,  $\underline{p}$ . Their dependence on  $\underline{E}$  and  $\underline{p}$  are shown heuristically, as follows.

Consider  $\underline{\alpha}$ , the number of new ion pairs formed per unit distance traveled by an ion. The ability of a particle such as an ion to cause further ionization depends upon the amount of energy it can furnish to the ionization process. A certain minimum energy is required to separate electrons from their atoms; this energy must be supplied from the kinetic energy of the ionizing particle. But this requires that the ionizing particle itself must have at least this minimum kinetic energy. To attain that kinetic energy, it must have been accelerated in an electric field, and the time required to acquire the velocity for that kinetic energy depends upon the field strength,  $\underline{E}$ , and the average distance traveled,  $\underline{s}$ , and therefore upon the product of  $\underline{E}$  and  $\underline{s}$ . Then in a fixed period of time, the greater this product, the more often ionizing ability is attained, and the greater is the number of new ions formed. But  $\underline{s}$ , the mean free path of the original ionizing particle, is inversely proportional to the gas pressure,  $\underline{p}$ . (In most of the writings on this subject, the temperature of the gas is ignored as being constant. In truth, the density of the gas is the controlling variable; but if the gas laws hold, pressure and density are directly proportional for constant temperature. Cf. Reference 15, pp. 82, 83.) Therefore, we have,

$$\alpha = f(E, p),$$

and it turns out that this is best expressed as

$$\frac{\alpha}{p} = F_1 (E/p). \quad (9)$$

Now consider  $\gamma$ , the average quantity of electrons emitted from the cathode for each positive ion bombarding the cathode. A minimum energy is required to remove an electron from the cathode material, and this energy must be supplied from the kinetic energy of the positive ions bombarding the cathode. Following the same general reasoning of the preceding paragraph for  $\alpha$ , we find that the quantity of electrons produced is again a function of the product of the electric field strength and the mean free path. Hence,

$$\gamma = f_2(E/p). \quad (10)$$

Both  $(\alpha/p)$  and  $\gamma$  have been determined experimentally as functions of  $(E/p)$  for many gases and cathode materials. These may be used in predicting the sparking potential,  $V_s$ , for a given electrode gap,  $d_s$ .

Solving Equation (7) for  $d$ , and substituting  $d_s$  for  $d$ ,

$$\epsilon^{\alpha d_s} = \frac{1}{\gamma} + 1 = \frac{1 + \gamma}{\gamma},$$

or

$$d_s = \frac{1}{\alpha} \log_{\epsilon} \frac{(1 + \gamma)}{\gamma}. \quad (11)$$

Multiplying by

$$E = \frac{V_s}{d_s} \quad (12)$$

$$V_s = \frac{E}{\alpha} \log_{\epsilon} \frac{(1 + \gamma)}{\gamma}.$$

Thus, using experimentally determined values of  $\alpha$  and  $\gamma$ , the sparking potential for any  $E$  may be predicted.

D. Paschen's Law (Reference 15, pp. 82, 96-100)

Paschen's Law states that the sparking voltage for a uniform electric field is a function of the product of gas pressure and electrode gap distance,

$$V_s = F(pd).$$

This relationship is a direct consequence of Townsend's sparking criterion, Equation (8),

$$\gamma e^{ad} = 1.$$

Substituting in Equation (8) the expressions for  $\alpha$  and  $\gamma$  from Equations (9) and (10),

$$f_2(E/p) \exp \left[ (pd) f_1(E/p) \right] = 1.$$

Writing for the uniform field

$$E = V_s/d_s,$$

and substituting,

$$f_2(V_s/pd) \exp \left[ (pd) f_1(V_s/pd) \right] = 1. \quad (13)$$

Equation (13) shows that  $V_s$  is an implicit function only of  $pd$ . For any given value of the product  $pd$ , one and only one value of  $V_s$  is possible to make Equation (13) hold true. Then it may be stated immediately that

$$V_s = F(pd), \quad (14)$$

and we have Paschen's Law.

Paschen's Law for several different gases and plane parallel electrodes of various materials is illustrated in Figure I-3 (cf. Reference 14, p. 84, Figure 2.2). These examples are typical, showing u-shaped curves which open upwards. With

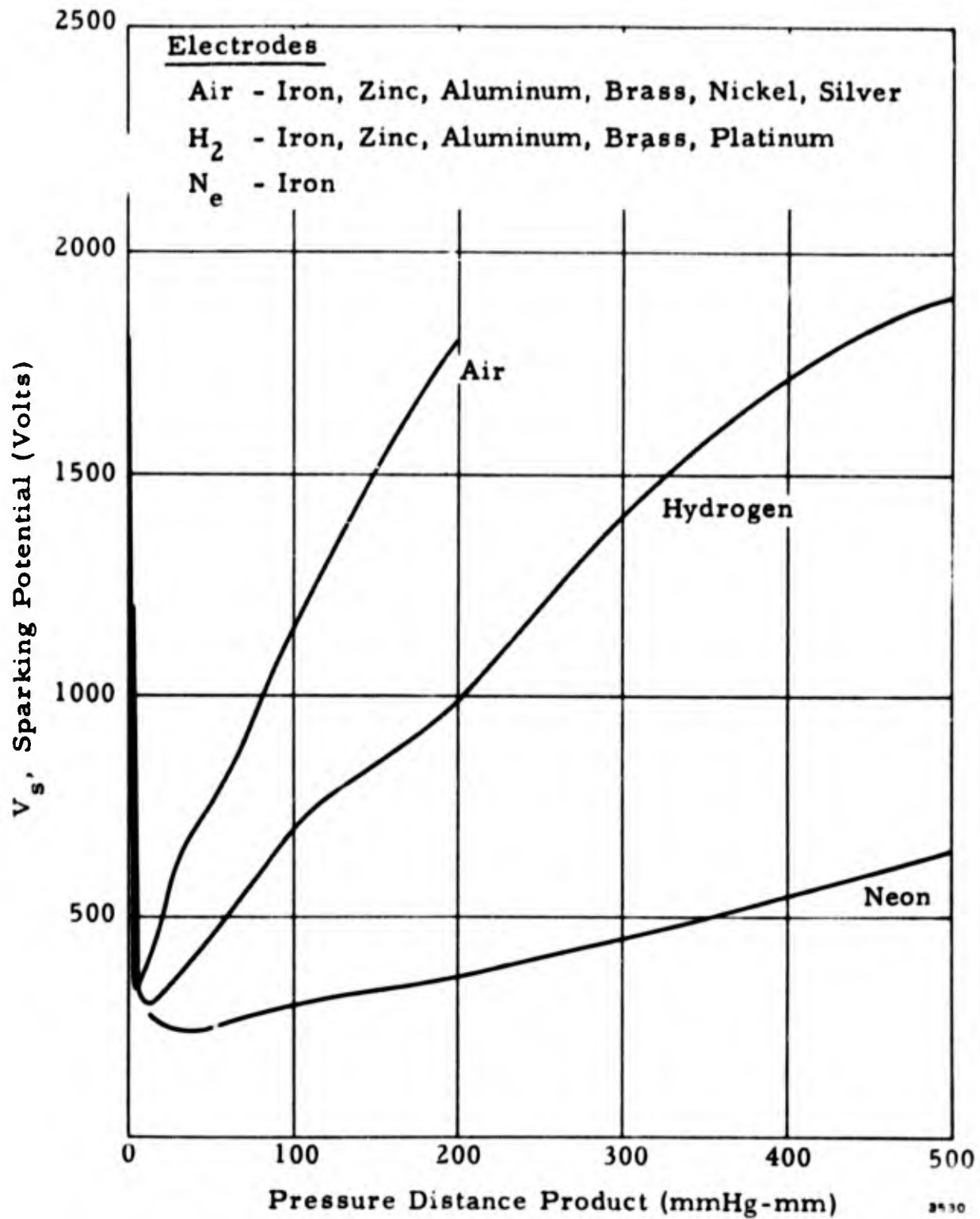


Figure I-3. Typical Breakdown Voltage Curves for Different Gases Between Parallel Plate Electrodes Illustrating Paschen's Law.

decreasing pressure-distance product,  $pd$ , the sparking voltage also decreases, approaching a minimum. With continued decrease of the  $pd$  product, the sparking voltage rises rapidly, theoretically increasing without bound as  $pd$  approaches zero. Actually, the phenomenon of field emission of electrons from the cathode will cause another type of electrical discharge to occur when the electric field strength becomes great enough, and Paschen's Law is then no longer applicable (see Reference 15, pp. 118-126). This is beyond the scope of this appendix.

Deviations from Paschen's Law have been examined carefully by experimentation. The deviations are such that the breakdown potential found for a large electrode gap and low pressure is higher than predicted from the data for a shorter gap and higher pressure. The minimum sparking potential,  $V_{\min}$  found for a particular product,  $p_0 d_0$ , is not affected by these deviations to any appreciable extent. The deviations have been studied by stating Paschen's Law in a more general form:  $V_s = F(p^m d^n)$ . This may in turn, be written  $p^m d^n = G(V_s)$ . Then, holding  $V_s$  constant, we may write

$$m \log p + n \log d = K$$

where

$$K = \log G(V_s) = \text{a constant} .$$

If  $m$  and  $n$  are constants, this is an equation of a straight line. Solving for  $\log p$ , we find the slope of the straight line to be  $-n/m$ :

$$\log p = - \left( \frac{n}{m} \right) \log d + \frac{K}{m}$$

This is illustrated in Figures 7 and 8 in which  $\log p$  is plotted as a function of  $\log d$ . If Paschen's Law holds,  $n$  should equal  $m$ , and the resulting curve should be a straight line with a slope equal to  $-1$ . If deviations occur, the slope is not equal to  $-1$ .

Solving for  $\log p$ , Paschen's Law may be checked statistically. The following null hypothesis and its alternative are stated:

$$H_0 : \frac{n}{m} = -1$$

$$H_1 : \frac{n}{m} \neq -1$$

Actually, published representative experimental slopes have been found to vary from  $-1.03$  to  $-1.19$ , showing that small deviations from Paschen's Law do exist. The best physical explanation appears to be that more ions diffuse to the external environment when the electrode spacing is increased. Therefore, with greater spacing, a higher voltage difference is necessary for the extra ionization to replace the lost ions before Townsend's sparking criterion is achieved. If the area of the flat, parallel electrodes were great enough compared with the gap, and if the pressure were low enough, ion diffusion would be negligible so that Paschen's Law would hold nearly exactly.

E. Nonuniform Electric Field (Reference 15, pp. 100-111)

The preceding development of Paschen's Law was based upon a uniform electric field, which is seldom found except in carefully controlled laboratory conditions. The development of Townsend's criterion for sparking from the Townsend equation was also based on the assumption that the first Townsend coefficient,  $\alpha$ , remains constant across the electrode gap for a given gap potential difference. Hence, both Paschen's Law and Townsend's sparking criterion require modification if the electric field is nonuniform, which is always the case for any electrodes except flat, parallel planes.

If  $\underline{E}$  is a function of the path between the electrodes, then  $\alpha$  is also, so that Equation (2) must be integrated as

$$\alpha = \exp \left( \int_{x_1}^{x_2} \alpha dx \right) \quad (15)$$

If the proper mathematical operations are carried out, this leads to a modified Townsend sparking criterion of more general application, in the form

$$\gamma \left[ \exp \left( \int_{x_1}^{x_2} \alpha dx \right) - 1 \right] = 1 \quad (16)$$

where

$$\alpha = g(E/p) \quad (17)$$

in which

$$E = h(V, x) . \quad (18)$$

In a gas at very low pressure, we may assume negligible alteration of the electric field at any particular location due to the presence of ions, except in very close proximity to each ion. Although this assumption may often not be justified except in a very gross sense, it will allow the establishment of an altered form of Paschen's Law. If the assumption holds, so that increase of ionization by increasing applied voltage does not in itself alter the electric field characteristics, then Equation (18) may be restated with  $\underline{V}$  as a simple multiplying factor:

$$E = Vh'(x) . \quad (19)$$

Hence,

$$\alpha = Vg'(x, 1/p) .$$

But it is reasonable to assume that the pressure  $\underline{p}$  is independent of the geometry of the electrodes, so that  $\underline{\alpha}$  becomes

$$\alpha = \frac{V}{p} g''(x) . \quad (20)$$

Recalling that  $\underline{\gamma}$  is

$$\gamma = f_2(E/p) , \quad (21)$$

and substituting Equation (19),

$$\gamma = f_2 \left[ (V/p)h'(x) \right] . \quad (21)$$

Now substituting Equations (20) and (21) in Equation (16),

$$f_2 \left[ (V_s/p)h'(x) \right] \left[ \left\{ \exp (V_s/p) \int_{x_1}^{x_2} g''(x)dx \right\} - 1 \right] = 1 . \quad (22)$$

Here,  $V_s$  is shown as an implicit function only of  $p$  and of the electrode geometry as defined by  $h'(x)$  and  $g''(x)$ . For any given electrode geometry, we may write

$$V_s = F \left[ p\phi(x) \right] , \quad (23)$$

where  $\phi(x)$  represents the geometric effects of both  $h'(x)$  and  $g''(x)$  .

In the case of parallel flat electrodes,  $\phi(x)$  becomes

$$\phi(x) = d$$

and Equation (23) reduces to Paschen's Law,

$$V_s = F(pd) .$$

For other electrode configurations, no such simplification is possible. However, it is reasonable to assume that some minimum sparking voltage will obtain for some particular value of pressure,  $(p_0)$  in a given electrode configuration. If such a set of circumstances exists, we may say that  $\phi(x) = d_0$  , an arbitrary constant determined by the geometry; and the minimum sparking potential is given by

$$V_{\min} = F(p_0 d_0) . \quad (24)$$

Thus, if the assumptions hold true that the ions do not alter the electric field characteristics, and that the geometric effects of electrode configuration on  $\alpha$  and  $\gamma$  are independent of  $V$  and  $p$ , then a minimum sparking potential should exist. Deviations from such a minimum will be large or small according to the degree of unreliability of these assumptions. For any given electrode configuration, it may be expected that deviations from the minimum sparking potential will be confined within a very small region of the  $pd$  product.

#### F. Electrode Material and Gas Composition

Although this appendix is concerned mainly with electrical discharges in air, some consideration should be given to electrical breakdown of gases which may be released by the materials used and to the use of various electrode materials.

The value of the first Townsend coefficient  $\alpha$ , is dependent upon the composition of the gas. The number,  $\alpha$ , of new ion pairs formed per unit distance traveled by an existing ion not only depends upon  $E$  and  $p$ , but upon the physical characteristics of the gas itself. The minimum energy required to remove an electron from an atom is determined by the ionization potential of the chemical element. The probability that an ionizing collision will occur if the energy is available depends on the distribution of electric fields around the atom due to its planetary electrons and upon the length of time the original ion remains in the vicinity of the atom. These and other considerations are lumped together in the ionization cross section of the gas, which is itself a function of the chemical composition of the gas. The effects of different gases on Paschen's Law are illustrated in Figure I-3.

The second Townsend coefficient,  $\gamma$ , is a function both of the gas and of the cathode material. It is a function of the gas primarily because of the difference in atomic mass of the different chemical elements. A certain minimum energy is required to remove an electron from the surface of a cathode made of a given material. This energy must come from the kinetic energy of the positive ions bombarding the cathode and is dependent on the ionic mass and, therefore, on the atomic masses of the chemical elements

composing the gas. But the minimum energy required to remove an electron from the cathode varies with the cathode material. This energy is called the "work function" of the material and is affected greatly by the presence of small surface impurities. Therefore, the second Townsend coefficient is not only a function of  $E$  and  $p$ , but also upon the chemical compositions of the gas and of the cathode material. The effect of different cathode materials on the minimum sparking potential is illustrated in Figure I-4. (cf. Reference 15, Figure 2.10, p. 91.)

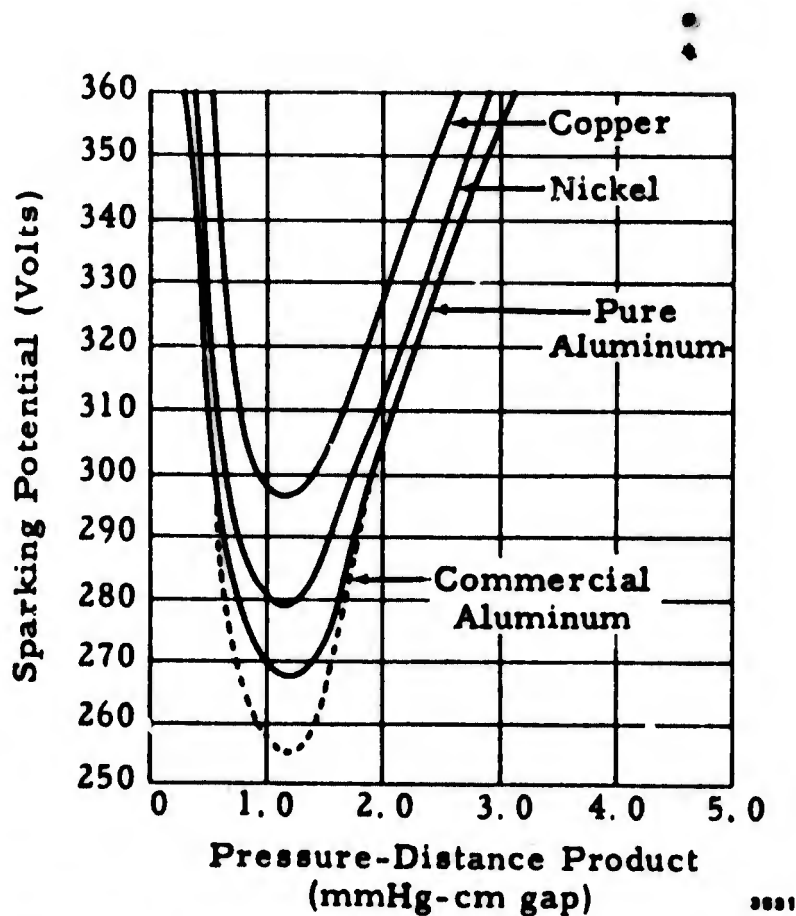


Figure I-4. Breakdown Voltage Curves for Different Cathode Materials in Hydrogen.

G. Cathode Potential Fall (Reference 14; Reference 26, pp. 73, 74, 82 through 86.)

Macmillan, Reference 14, has recommended the use of the cathode potential fall, or "cathode fall," as a safe criterion in establishing a maximum allowable

potential difference between exposed electrical conductors in low pressure air. The cathode fall,  $\underline{V_c}$ , is the potential drop in the cathode dark space of a glow discharge, and most of the potential drop in a glow discharge occurs in this region. The cathode potential fall in a "normal" glow discharge is independent of the gas pressure, the electrode configuration, and the total applied voltage. (A "normal" glow discharge exists if the cathode glow does not cover the entire cathode area.) As the electrode potential is decreased, the ionization current decreases, but the cathode potential fall remains constant. At some potential still greater than the cathode fall, the total applied potential is insufficient to maintain the glow discharge, and it is extinguished. Hence, the cathode fall potential,  $\underline{V_c}$ , is a safe maximum potential which is lower than the minimum potential to maintain a discharge. But the minimum voltage required to initiate a discharge,  $\underline{V_{min}}$ , is always equal to or greater than that required to maintain the discharge, so that  $\underline{V_c}$  is actually a doubly safe criterion.

$\underline{V_c}$  is a function of the gas and of the cathode material, and varies widely for different combinations. However, the main concern here is about the initiation of glow discharges in air. Macmillan has tabulated values of  $\underline{V_c}$  for several common materials in air; these are reproduced in Table 1. It will be noted that

Table 1. Normal Cathode Fall in Air.

Cathode Material	Cathode Fall in Volts	Cathode Material	Cathode Fall in Volts
Al	229	Mg	224
Ag	280	Na	200
Au	285	Ni	226
Bi	272	Pb	207
Cd	266	Pd	421
Co	380	Pt	277
Cu	370	Sb	269
Fe	269	Sn	266
Ir	380	Zn	277
K	180		

the lowest value of  $V_c$  for any material likely to be exposed to air in a missile or other vehicle is due to the use of lead in solder alloys. No data are available for  $V_c$  for the solder alloys themselves, but the value for lead is the lowest of all those elements used in solder. Macmillan assumed that 200 volts could be used as a conservative maximum allowable pin-to-pin voltage for connectors using air as dielectric. This seems to be a reasonable assumption and may be applied equally well as a criterion for the maximum allowable potential between any conductors in air.

Any arbitrary safety criterion, such as the 200 volts criterion above, is subject to limitations which may not be at all obvious. Perhaps the most serious limitation here is that a possibility may exist for transition of a corona to an arc. The major difference between the glow discharge and the arc is in the mechanism of generating electrons to maintain the current. In the glow discharge, most of the electrons are emitted from the cathode because of positive ion bombardment. In the arc, sufficient energy is available to raise the cathode temperature until thermionic emission of electrons is the major source of ions. (Reference 11, pp. 247-253.) If the circuit impedance is low enough, the arc discharge may be maintained at a voltage very much lower than  $V_c$ . Once an arc is initiated, it will be maintained until the circuit impedance is made high enough that insufficient energy is supplied to the arc to continue the thermionic emission of electrons.

APPENDIX II

ALTITUDE-PRESSURE CONVERSION TABLE

The following table is based on 1958 data obtained from SPUTNIK.

<u>Altitude (Feet)</u>	<u>Pressure (mm Hg)</u>
0	760.0
10,000	522.73
20,000	349.25
30,000	226.10
40,000	141.20
50,000	87.50
60,000	54.20
70,000	33.60
80,000	20.90
90,000	13.00
100,000	8.30
110,000	5.40
120,000	3.50
130,000	2.40
140,000	1.60
150,000	1.10
160,000	0.76
170,000	0.53
180,000	0.37
190,000	0.25
200,000	0.17
210,000	0.11
220,000	0.073
230,000	0.047
240,000	0.029
250,000	0.017
260,000	0.010

1000 Microns Hg = 1 mm Hg

APPENDIX III  
STATISTICAL MODELS

A. Linear Regression

For a fixed voltage ( $V_0$ ), Paschen's Law in its generalized form may be expressed as

$$m \log p + n \log d = \log G(V_0) = K \quad (1)$$

or

$$\log p = -\frac{n}{m} \log d + \frac{K}{m} .$$

Substituting

$$\begin{aligned} y &= \log p \\ x &= \log d \\ a &= -\frac{n}{m} \\ b &= \frac{K}{m} \end{aligned} \quad (2)$$

Equation (1) reduces to

$$y = ax + b .$$

Given  $n$  paired observations,  $(x_i, y_i)$ ,  $i = 1, 2, \dots, n$ , the least squares fit to the linear Equation (3) may be obtained by minimizing

$$\sum_{i=1}^n (y_i - ax_i - b)^2 . \quad (4)$$

That is, the constants  $\underline{a}$  and  $\underline{b}$  must be chosen such that Equation (4) is a minimum. This is realized by taking partial derivatives with respect to  $\underline{a}$  and  $\underline{b}$  and setting these partial derivatives equal to zero.

I. e.,

$$\frac{\partial}{\partial b} \sum_{i=1}^n (y_i - ax_i - b)^2 = \sum_{i=1}^n (y_i - ax_i - b) (-2) = 0 \quad (5)$$

$$\frac{\partial}{\partial a} \sum_{i=1}^n (y_i - ax_i - b)^2 = \sum_{i=1}^n (y_i - ax_i - b) (-2x_i) = 0,$$

or

$$\sum_{i=1}^n y_i = a \sum_{i=1}^n x_i + nb \quad (6)$$

$$\sum_{i=1}^n x_i y_i = a \sum_{i=1}^n x_i^2 + b \sum_{i=1}^n x_i.$$

Solving for a and b and denoting their solutions by  $\hat{a}$  and  $\hat{b}$  respectively, the following are obtained.

$$\hat{a} = \frac{\begin{vmatrix} \sum y_i & n \\ \sum x_i y_i & \sum x_i \end{vmatrix}}{\begin{vmatrix} \sum x_i & n \\ \sum x_i^2 & \sum x_i \end{vmatrix}} = \frac{(\sum x_i)(\sum y_i) - n \sum x_i y_i}{(\sum x_i)^2 - n \sum x_i^2} = \frac{\sum (x_i - \bar{x})(y_i - \bar{y})}{\sum (x_i - \bar{x})^2} \quad (7)$$

$$\hat{b} = \frac{\begin{vmatrix} \sum x_i & y_i \\ \sum x_i^2 & \sum x_i y_i \end{vmatrix}}{\begin{vmatrix} \sum x_i & n \\ \sum x_i^2 & \sum x_i \end{vmatrix}} = \frac{(\sum x_i)(\sum x_i y_i) - (\sum y_i)(\sum x_i^2)}{(\sum x_i)^2 - n \sum x_i^2} = \bar{y} - \hat{a} \bar{x}, \quad (8)$$

where

$$\bar{x} = \frac{\sum x_i}{n},$$

and

$$\bar{y} = \frac{\sum y_i}{n} .$$

The linear equation representing the best fit to the  $n$  paired observations  $(x_i, y_i)$  is then

$$\hat{y} = \hat{a} x + \hat{b} . \tag{9}$$

**B. Prediction Interval for the Regression Line**

The estimated regression line,  $y = \hat{a} x + \hat{b}$ , based on a sample of  $n$  paired observations, serves only as an estimate of the actual regression line,  $y = ax + b$ . The measure of the error involved in predicting  $y$ , given  $x$ , say  $x_0$ , may be obtained by utilizing a prediction interval which is analogous to a confidence interval.

The following assumption is made. The variate  $y$  is a random variable with a normal distribution having mean  $a + bx_0$  and variance  $\sigma^2$ .

The predicted value  $y_0 = \hat{a} + \hat{b}x_0$  has two sources of error:

- (a)  $\hat{a}x + \hat{b}$  is merely an estimate of the mean of  $y$ .
- (b) The estimated mean is subject to random sampling errors inherent in  $\hat{a}$  and  $\hat{b}$ .

If  $\sigma$ ,  $a$ , and  $b$  were exactly known, the 90 per cent predicted interval for  $y$  would simply be

$$b + ax_0 - 1.645\sigma \text{ to } b + ax_0 + 1.645\sigma , \tag{10}$$

since the probability that  $y$  will fall within  $1.645\sigma$  of its mean is 0.90 for the normal distribution. Since all these parameters except  $x_0$  are unknown, the 90 per cent prediction interval in terms of their estimates is

$$\hat{b} + \hat{a}x_0 - A \text{ to } \hat{b} + \hat{a}x_0 + A , \tag{11}$$

where

$$A = (t_{n-2, 0.90}) S_{y|x} \sqrt{\frac{n+1}{n} + \frac{(x_0 - \bar{x})^2}{\sum (x_i - \bar{x})^2}} \quad (12)$$

with

$n$  denoting the sample size,  
 $t_{n-2, 0.90}$  denoting the point obtained from the  $t$  distribution with  $n - 2$  degrees of freedom and 90 per cent two-sided prediction interval and

$$S_{y|x} = \sqrt{\frac{\sum_{i=1}^n (y_i - \hat{a}x_i - \hat{b})^2}{n-2}} \quad (13)$$

### C. Statistical Test of Hypothesis on the Regression Slope

The following hypotheses are formulated with respect to the regression slope:

$$H_0: a = -1$$

$$H_1: a \neq -1$$

$H_0$ , our null hypothesis, states that the regression slope is equal to minus one. If  $H_0$  is rejected, the alternative hypothesis  $H_1$  which states that the slope is not equal to minus one must then be accepted. Conversely, if  $H_0$  is accepted, then  $H_1$  must be rejected.

The "decision rule" for accepting or rejecting  $H_0$  is based on the following inequalities:

$$|T| = \left| \frac{\hat{a} + 1}{S_{y|x}} \sqrt{\sum (x_i - \bar{x})^2} \right| \geq t_{n-2, 0.90} \quad (14)$$

$H_0$  is rejected at the 10 per cent significance level.

If

$$|T| < t_{n-2, 0.90}$$

$H_0$  is accepted.

D. Confidence Limits for the Regression Slope

The inequalities in

$$P(-t_{n-2, 0.90} < T < t_{n-2, 0.90}) = 0.90 \quad (15)$$

may be used to determine confidence limits for  $\hat{a}$ .

I. e.,

$$\begin{aligned} P(-t_{n-2, 0.90} < T < t_{n-2, 0.90}) &= P\left(-t_{n-2, 0.90} < \frac{\hat{a} - a}{S_{y|x}} \sqrt{\Sigma(x_i - \bar{x})^2} < t_{n-2, 0.90}\right) \\ &= P\left(\hat{a} - \frac{(t_{n-2, 0.90}) S_{y|x}}{\sqrt{\Sigma(x_i - \bar{x})^2}} < a < \hat{a} + \frac{(t_{n-2, 0.90}) S_{y|x}}{\sqrt{\Sigma(x_i - \bar{x})^2}} = 0.90\right). \end{aligned} \quad (16)$$

The confidence limits for "a" are then

$$\hat{a} - \frac{(t_{n-2, 0.90}) S_{y|x}}{\sqrt{\Sigma(x_i - \bar{x})^2}} \quad \text{for the lower limit,} \quad (17)$$

and

$$\hat{a} + \frac{(t_{n-2, 0.90}) S_{y|x}}{\sqrt{\Sigma(x_i - \bar{x})^2}} \quad \text{for the upper limit.} \quad (18)$$

## BIBLIOGRAPHY

1. Altshuler, S., M. M. Moe, and P. Molmud. "The Electromagnetics of the Rocket Exhaust." Space Technology Laboratories, Inc. GM-TR-0165-00397. 15 June 1958. (C).
2. Brown, S. C. "High Frequency Gas-Discharge Breakdown." Proc. IRE, 39 (December 1951), 1493-1501.
3. Chown, J. B., W. E. Scharfman, and T. Morita. "Voltage Breakdown Characteristics of Microwave Antennas." Proc. IRE, 47 (August 1959), 1331-1337.
4. Cobine, J. D. Gaseous Conductors, Theory, and Engineering Applications, New York: Dover Publications, 1958.
5. Crawford, F. W., and W. A. Gambling. "Minimum Spark Breakdown and Glow Voltages." Canad. J. Phys., 35, Pt. I, (January-June 1957), 562-568.
6. Gould, L. "Handbook on Breakdown of Air in Waveguide Systems," Reprint of Navy Index No. NE-111616, as published by Microwave Associates, Inc., Burlington, Mass.
7. Gould, L., and T. W. Roberts. "Breakdown of Air at Microwave Frequencies." J. Appl. Physics, 27 (October 1956), 1162-1170.
8. Guthrie, A., and R. K. Wakerling, eds. Characteristics of Electrical Discharge in Magnetic Fields. New York: McGraw-Hill Book Company, Inc.,
9. Flügge, S., ed. Handbuch der Physik. Berlin: Springer, 1956. 21 Electron-Emission, Gas Discharges I; 22, Gas Discharges II.
10. Hart, G. K., F. R. Stevenson, and M. S. Tanenbaum. "High Power Breakdown of Microwave Structures." IRE Convention Record. Pt. 5, pp. 199-203.
11. Holm, R. Electric Contacts. Stockholm: Hugo Gebers, 1946.
12. Loeb, L. Basic Processes of Gaseous Electronics. Berkeley: The University of California Press, 1955.
13. MacDonald, A. D. "High Frequency Breakdown in Air at High Altitude." Proc. IRE, 47 (March 1959), 436-441.
14. Macmillan, R. S. "Voltage Ratings for Electrical Connectors Subjected to Low-Pressure Environments." Letter Report to R. W. Williams, Space Technology Laboratories, Inc., 19 August 1957.

15. Meek, J. M. and J. D. Craggs. Electrical Breakdown of Gases. Oxford: The Clarendon Press, 1953.
16. Molmud, P. "The Pressure Characteristics of Microwave Breakdown," Space Technology Laboratories, Inc. GM-47.4-13.
17. Molmud, P. "The Altitude Dependence of Radar Signal Loss." Space Technology Laboratories, Inc. GM-47.4-12. 3 June 1958. (C).
18. Nottingham, W. "Bibliography on Physical Electronics." M.I.T. Addison-Wesley Printing Company, 1959. 1-133.
19. Pasha, R. A. "VHF Breakdown of Air at Low Pressures." Ballistics Res. Labs. Rept. 944. August 1955.
20. Prowse, W. A. "The Initiation of Breakdown in Gases Subject to High Frequency Electric Fields." J. Brit. Inst. Radio Eng., 10 (November 1950), 333-346.
21. Redelsheimer, A. C. "Extinction Voltage on AN3106E-22-14 at 60 cps, 400 cps, and 1000 cps." Convair Astronautics, Memorandum REL 493, 27 August 1957.
22. Reed, A. C. "Literature Survey-Low Pressure Electrical Discharge." Space Technology Laboratories, Inc. GM-40.2-238. 19 September 1958.
23. Rose, D. J. and S. C. Brown. "Microwave Gas Discharge Breakdown in Air, Nitrogen and Oxygen." J. Appl. Physics, 28 (May 1957), 561-563.
24. Skellett, Firth, Mayer. "The Magnesium Oxide Cold Cathode and its Application in Vacuum Tubes." Proc. IRE, 47 (October 1959), 1704-1712.
25. Sterne, T. E., B. M. Folkart, and G. F. Schilling. "An Interim Model Atmosphere Fitted to Preliminary Densities Inferred from U. S. S. R. Satellites." Smithsonian Contributions to Astrophysics, 2 (1958), 275-279.
26. Stranathan, J. D. The Particles of Modern Physics. Philadelphia: The Blakistone Co., 1942.
27. Von Engel, A. Ionized Gases. Oxford: Clarendon Press, 1955.
28. Worth, F. "A Study of Voltage Breakdown in the Cavity Fed Slot Antenna." Lockheed Aircraft Corp. Missile Systems Division. MSD 20, 30 January 1957.
29. Wright Air Development Center. "Design Factors for Aircraft Electronic Equipment." WADC Technical Report 56-148, AD-142 204. 5, 40-43.
30. Spink, B. R. "A Practical Solution to the Arcing Problem at High Altitudes." AC Spark Plug Div., GMC. Eng. Memo. Rpt. EMR 4-373. 10 August 1959.

### ACKNOWLEDGEMENT

We wish to acknowledge the assistance of Frank Nishime in the preparation of this report. He supplied the statistical methods as outlined in Appendix III, applied them to the data, and prepared the statistical tables. His work was a prerequisite for arriving at certain conclusions.

DISTRIBUTION

J. H. Allen	R. Luck
G. D. Bagley	W. F. McGrath
E. W. Banios	P. Molmud
M. Barbe	S. C. Morrison
N. Christensen	J. R. Penning
F. Cooper	H. R. Powell
J. L. Coulson	A. C. Reed (25)
D. H. Crothers	J. P. Rudnick
W. A. Dodge (2)	W. T. Russell
H. Hayes	Y. Shibuya
L. Hirschl (3)	M. H. Shuler
L. A. Hoffman	T. D. Smith
I. M. Holliday (3)	J. D. Sorrels
P. V. Horton	W. A. Stewart
H. G. Kasten	A. K. Thiel
R. D. Kennedy	J. E. Vehrencamp
F. P. Klein	J. F. Vogl
W. H. Krebs (40)	H. C. Yost
L. K. Lee	STL Library (3)
F. C. Loesch	